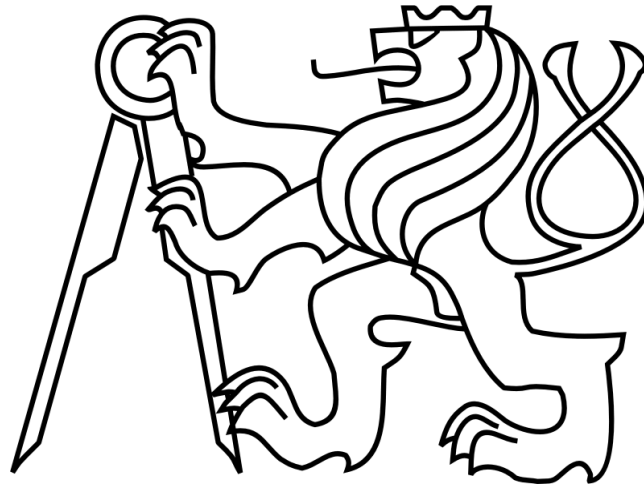# Czech Technical University in Prague

Faculty of Electrical Engineering

Department of Circuit Theory

Simulation and Hardware Modeling of a Real BLDC Motor Applicable in Medicine

Master's thesis

Author: Bc. Martin Bulán

Supervisor: Ing. Jiří Maršík Ph.D.

České vysoké učení technické v Praze
Fakulta elektrotechnická

Katedra teorie obvodů

ZADÁNÍ DIPLOMOVÉ PRÁCE

Student: Bc. Martin B u l á n

Studijní program: Biomedicínské inženýrství a informatika (magisterský)

Obor: Biomedicínské inženýrství

Název tématu: Počítačová simulace a tvorba modelu reálného BLDC motoru
použitelného v lékařství

Pokyny pro vypracování:

1. Zmapování a porovnání současné problematiky simulace a modelování DC a BLDC motorů v lékařství.
2. Vlastní návrh počítačového modelu vybraného BLDC motoru využitelného v lékařském prostředí za využití současných softwarových nástrojů.
3. Tvorba reálného modelu BLDC motoru pro:
   - porovnání s průmyslově vyráběným motorem
   - vyhodnocení kvality zvolené řídicí jednotky motoru pomocí vybraných parametrů
4. Ověření vlastností vytvořeného modelu.

Seznam odborné literatury:

[1] V. Hrabovcová, P. Rafajdus, M. Franko, P. Hudák: Meranie a modelovanie elektrických strojov. Žilinská univerzita, 2008.
[2] A. Tashakori, M. Ektesabi, N. Hosseinzadeh: Modeling of BLDC Motor with Ideal Back-EMF for Automotive Applications. Londýn, 2011.
[3] M. Ložek, P. Zahradník, J. Havlík: Regulace BLDC pohonů pro asistivní technologie. Trendy v biomedicínském inženýrství, Rožnov pod Radhoštěm, 2011.
[4] A. K. Daud: Brushless D.C. Motor for Medical Applications. Palestine Polytechnic University, Palestine. 2010.

Vedoucí diplomové práce: Ing. Jiří Maršík, Ph.D.

Platnost zadání: do konce letního semestru 2014/2015

L.S.

prof. Ing. Pavel Sovka, CSc.   prof. Ing. Pavel Ripka, CSc.
vedoucí katedry   **děkan**

V Praze dne 10. 1. 2014

Czech Technical University in Prague
Faculty of Electrical Engineering

Department of Circuit Theory

DIPLOMA THESIS ASSIGNMENT

Student: Bc. Martin   B u l á n

Study programme: Biomedical Engineering and Informatics

Specialisation: Biomedical Engineering

Title of Diploma Thesis: Simulation and Hardware Modeling of a Real BLDC Motor
Applicable in Medicine

Guidelines:

1. Mapping and comparison today's issues of simulation and modeling of DC and BLDC motors in medicine.
2. Designing a computer model of a specific BLDC motor applicable in a medical environment, using current software tools.
3. Hardware model of selected BLDC motor:
    - Comparison with a manufactured motor
    - Evaluating quality of a specific motor control unit using selected parameters
4. Verification of the model properties.

Bibliography/Sources:
[1] V. Hrabovcová, P. Rafajdus, M. Franko, P. Hudák: Meranie a modelovanie elektrických strojov. Žilinská univerzita, 2008.
[2] A. Tashakori, M. Ektesabi, N. Hosseinzadeh: Modeling of BLDC Motor with Ideal Back-EMF for Automotive Applications. Londýn, 2011.
[3] M. Ložek, P. Zahradník, J. Havlík: Regulace BLDC pohonů pro asistivní technologie. Trendy v biomedicínském inženýrství, Rožnov pod Radhoštěm, 2011.
[4] A. K. Daud: Brushless D.C. Motor for Medical Applications. Palestine Polytechnic University, Palestine. 2010.

Diploma Thesis Supervisor: Ing. Jiří Maršík, Ph.D.

Valid until: the end of the summer semester of academic year 2014/2015

L.S.

prof. Ing. Pavel Sovka, CSc.   prof. Ing. Pavel Ripka, CSc.
  Head of Department   **Dean**

Prague, January 10, 2014

Prohlášení autora práce

Prohlašuji, že jsem předloženou práci vypracoval samostatně a že jsem uvedl veškeré použité informační zdroje v souladu s Metodickým pokynem o dodržování etických principů při přípravě vysokoškolských závěrečných prací.

V Praze dne ……………………….   ………………………………………….............
                                                                              Podpis autora práce

Contents

Abstract

BLDC motors are nowadays emerging in most fields of development. One of those fields is also biomedical engineering. This area has very specific requirements on the motors, because the devices, in which the motors are integrated, can often safe a human life. The goal of this thesis is to find out, what tools are currently available to model a brushless DC motor applicable in medicine and to use one of those tools to create a software model of a real motor. For this task it is also necessary to fully understand the principles of the BLDC and its control. Next task is to design a hardware model of the motor. This device is then compared with a real motor and used as a reference for industrial BLDC control units evaluation. The advantage of the reference is the stability of its electrical parameters. Since it has no parts which mechanically move, it can be used as an etalon for long term testing of the control units stability.

Abstrakt

BLDC motory se v současné době vyskytují téměř ve všech oblastech vývoje. Jedním z těchto oborů je také biomedicínské inženýrství. Toto odvětví má velmi specifické požadavky, protože přístroje, do kterých jsou tyto motory integrovány, často zachraňují lidské životy. Cílem této práce je zjistit, pomocí kterých nástrojů je dnes možné namodelovat stejnosměrný bezkartáčový motor a pomocí jednoho z těchto nástrojů vytvořit softwarový model reálného motoru. Pro tento úkol je nutné plně pochopit principy funkce BLDC a jeho řízení. Dalším úkolem je návrh hardwarového modelu motoru. Toto zařízení je poté porovnáno se skutečným motorem a použito jako reference pro ohodnocení průmyslových řídicích jednotek. Hlavní výhoda spočívá ve stabilitě jeho elektrických parametrů. Protože reference nemá mechanicky pohyblivé části, může být použita jako etalon pro dlouhodobé testování stability řídicích jednotek.

Acknowledgement

I would like to thank my supervisor Jiří Maršík for all his help, mentoring and inspiration and the company Robert Bosch České Budějovice for providing me everything I needed to work on my thesis. I would also like to thank my family for all the support they gave me during my studies.

List of abbreviations

DC   Direct Current

BLDC   Brushless DC

VAD   Ventricular Assist Device

LVAD   Left Ventricular Assist Device

RVAD   Right Ventricular Assist Device

BiVAD   Biventricular Assist Device

CPAP   Continuous Positive Airway Pressure Device

ECT   Emission Computed Tomography

SPECT   Single Photon Emission Computed Tomography

MOSFET   Metal–Oxide–Semiconductor Field-Effect Transistor

EMF   Electromagnetic Field

FEA   Finite Element Analysis

NI   National Instruments

FPGA   Field-Programmable Gate Array

HIL   Hardware In the Loop

RMS   Root Mean Square

GUI   Graphical User Interface

CCU   Customer's Control Unit

ICU   Internal Control Unit

USB   Universal Serial Bus

PWM   Pulse-Width modulation

RPM   Revolutions Per Minute

1 Introduction

Electrical motors are nowadays installed in basically every area of modern technology. A very significant subset of electrical motors are DC motors (direct current). This kind of electrical machines is manufactured in the size from the smallest, dedicated for small mechanics, to the largest, used above all in the industry or public transportation. DC motor is consisted of two main parts: the stator and the rotor. Stator is basically just a one or multiple-pole permanent magnet, which creates a permanent magnetic field inside the machine. Rotor is a coil, which generates a magnetic field through an electrical current flowing from one of its poles to another. Thanks to the interaction of those two fields, a mechanical torque emerges on the rotor, which works against an external load, the motor's friction and the moment of inertia [3][33].

Of course, since the permanent magnet of the stator creates a static magnetic field, the magnetic field of the rotor must change periodically so as to keep the rotor moving. This is achieved by electrical commutation of the rotor's winding. An electrical potential is brought to the motor's clamps. Thanks to the brushes at the boundary of the static skeleton of the machine and the rotor's contacts, the winding is always supplied with an electrical current [33]. As the rotor keeps turning, the contacts on the brushes switch periodically, which causes changing the current direction with every half of the rotational period [3].

This principle has the advantage of simplicity, which helped the DC motors reach a high popularity amongst the designer engineers. It has, however, also some disadvantages, which eventually made the developers come up with some new solutions. First and the biggest disadvantage are the brushes. If the motor is not constructed well enough, the brushes can be short-circuited, which can cause a fatal damage to the motor or the power source (with a high current, the contacts get overheated and can weld the rotor to the motor's skeleton). This can be avoided by putting a small gap between the contacts, preventing the brushes to connect without a proper load. The wider the gap is, the more stable the motor is. It causes, however, a negative effect called a torque ripple – periodical changes of the mechanical moment incurred due to short disconnection of the winding from the power source during the commutation phase. Next problem with the

brushes is that they decrease the lifespan of the whole motor because the contacts mechanically wear out sooner [20][3].

All those negatives lead the engineers to find a different way, where they would not have to use the brushes. One of the solutions is the BLDC motor (brushless DC). Compared with the classical DC motor, BLDC has some significant differences, bringing a whole new spectrum of advantages. But those differences also make some troubles connected to the new technology that did not need to be dealt with before.

The main difference is that, unlike by the DC motor, the BLDC has the permanent magnet on its rotor and the variable magnetic field is created by the stator. This is a big plus since there is no need to transfer the electrical energy to the rotor anymore, which allows us to leave out the brushes from the concept. Without the brushes, the lifespan of the motor is increased significantly and the motor has a smaller internal friction [20][3].

Next difference is the 3-phase principle of the BLDC. The DC machine has only one coil on the stator, creating the magnetic field. To the contrary, the BLDC uses three coils, each for one phase [22].

Since the BLDCs are currently applied increasingly in most areas, it became necessary to create software models for early stages of testing because it would lower the costs for the development greatly. There are many ways how to approach the problem of simulation. For example heating of the motor can be a big issue and it is a typical parameter which can be simulated. Apart from the heat stability, the motor also has to fulfill mechanical strength, maximum torque or angular velocity requirements and others.

Very important set of parameters are also the electrical parameters like nominal current, supply voltage, active power and others [32]. Also those parameters must be simulated. It is, however, better to use a slightly different approach. The way those parameters can be obtained is not only via a software tool but it can be also simulated through a hardware tool, which acts like a motor, but has no mechanical parts affecting the electrical parameters. This particular piece of hardware then does not only allow measuring the parameters but it can also work as a reference part for the control units because its characteristics do not change so rapidly.

2 Main targets of the thesis

This thesis deals with a computer simulation and a design of a hardware BLDC model used in biomedical and industrial environment. First, it is necessary to completely understand the principles of this type of electrical motor and its modeling.

In today's technical world, the right choice and following use of simulation tools for visual representation of the connection between mechanical and electrical part of the system is essential.

The target of this thesis is using the knowledge about the BLDC motor and the issues of its control acquired from the software model to create a hardware model, which would serve as a reference part for evaluation of industrial control units.

This hardware reference then must be compared with real motors (above all the stability of its parameters is vital) and then used for a comparison of multiple control units and related evaluation.

3 Overview of the problem

In this chapter I would like to describe the biggest issues of application of the BLDCs in medical environment. After that I have prepared some typical examples of the use of brushless DC motors in medicine. I have tried to show examples from multiple medical areas like cardiology, nephrology, dentistry, medical mobility and others so it would be clear that BLDC motors are already widely used without any significant troubles. Next part of this chapter is a description of the BLDC principles and the issues of its control. This knowledge is vital for the last part of this section where current simulation possibilities of this technology are described.

3.1 Medical application of the BLDC

3.1.1 Specific requirements of the medical device industry

Biomedical engineering is a very specific area regarding the requirements on the motor's parameters. First of them is electrical efficiency. Many medical devices require to be powered by batteries, which is still a big weakness of most electrical systems. Even modern high capacity batteries are not very hard to discharge and so electrical consumption as low as possible is needed especially by the electromechanical elements of the device. Since the BLDC has no brushes, it has lower viscous friction which together with more efficient control algorithm can cause a significant power saving [6][23].

Next thing the motor has to fulfill is to be very silent. Healthcare facilities have very low noise level standards, because for most patients the silence is one of the most important cures. For this reason, a device with an electrical motor ought not to be, in an ideal case, heard at all.

Since the medical devices are often very hard and expensive to repair, it is also necessary for them to last as long as possible. In extreme cases, a surgery would be necessary to fix the motor (heart assist systems). For this reason, longer lifespan of all parts of the device must be requested. As explained in Chapter 1, the BLDC can easily outmatch the standard DC motor in this discipline. According to [6] and [7], the BLDC's lifespan is 2-4 times longer than a DC machine.

Last requirement worth to mention is that the motor must be often spark-free. In many cases the medical devices have to work in an oxygen-rich environment. Using a DC motor for such application would be very dangerous due to their inclination to sparkle on the brushes during the commutation phase, which could even cause in such surroundings an explosion. For this reason, a BLDC is preferred for instruments like this.

3.1.2   Ventricular assist device

Ventricular assist device (VAD) is a system designed to support or in some cases even replace a failing heart. There are three types of the VAD – left ventricular assist device (LVAD)(Figure 1), right ventricular assist device (RVAD) and the previous two combined (BiVAD). This short-term circulatory support is above all indicated for patients with a rapid heart failure. It can help during the surgery and later as a support for recovery. It gives more time to the patients waiting for a heart transplant. The VAD is usually prescribed, when one or both ventricles (the lower chambers of the heart) stop working. This may be after a heart surgery, when it is just supposed to help the heart recover or it can replace the heart permanently (for patients who are not eligible for a heart transplant). However it is mostly used as a bridge for a heart transplant because the patients with a fatal heart disease often have to wait too long before a proper donor is found. The VAD in this case helps to survive this period and clears the patient's way to a normal life [24][25].

The principle of the VAD is quite simple. There is one tube carrying blood to the pump and another tube which carries it back under a required pressure. The pump has a power source, which is connected to a control unit. This unit operates the pump, measures the supply voltage and gives a warning, when anything goes wrong. There are two kinds of the pump. First one generates a pulsatile blood flow more similar to the healthy heart behavior. The other one keeps the continuous flow of blood. It is hard to tell which one is better for the patient because there have not been enough research to decide. However, in both cases the body gets enough blood to survive [25].

The most widely used type of VAD is the LVAD. It is connected to the left ventricle and pumps the blood to the aorta – the main artery, which supplies the body with an oxygen-rich blood. On the other hand, the RVAD is pumping the blood from the right ventricle to the pulmonary artery (this artery carries the blood to the lungs to pick

up oxygen). Unlike the LVAD, the RVAD is usually used only as a support after the LVAD or other kind of heart surgery. The BiVAD is used, when both ventricles need an external help. This solution can also be replaced with a completely artificial heart[25].
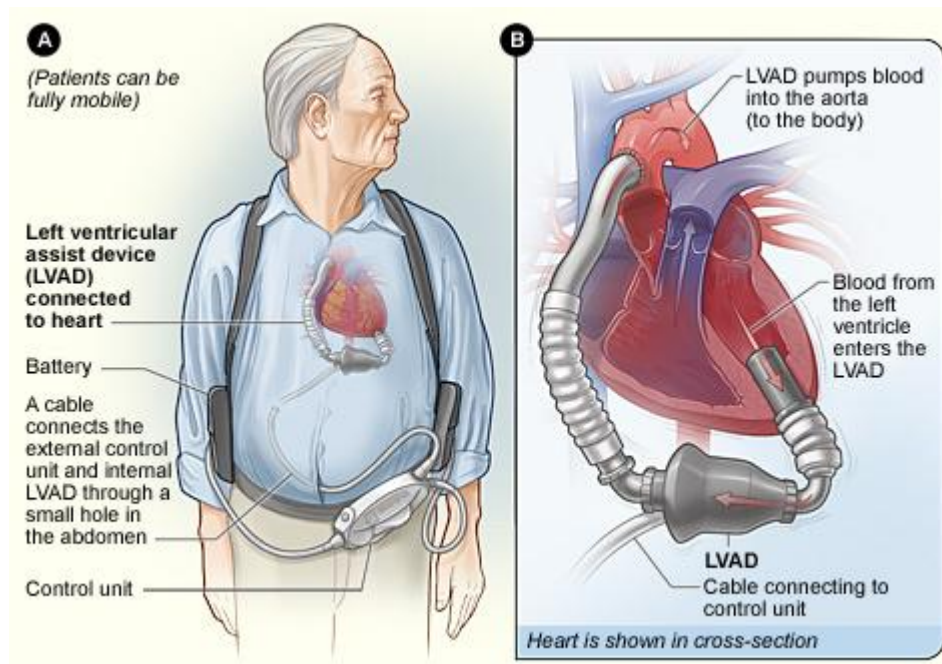

Figure 1 Connection of an implantable LVAD [25]

Another way to classify the VAD is whether it is located outside the patient's body (Figure 2), connected via tubes or it is surgically placed inside the body. The first one is called a transcutaneous VAD and the tubes are connected to the heart through small holes in the patient's abdomen. It is mostly used as a short-term solution after a surgery, because the patient's mobility is in this case very limited. An implantable VAD is located inside the body. However, its battery and control unit are still located outside the body. The implantable VAD is used as a long term solution. Although it does not completely substitute a real heart, it can significantly improve the patient's life, who is able to, to a certain degree, live as a healthy person.

Although the VAD is often a very good solution for a heart failure treatment, there are still cases when it cannot be used. For example an acute kidney failure, brain injury or an infection are considered as a contraindication.
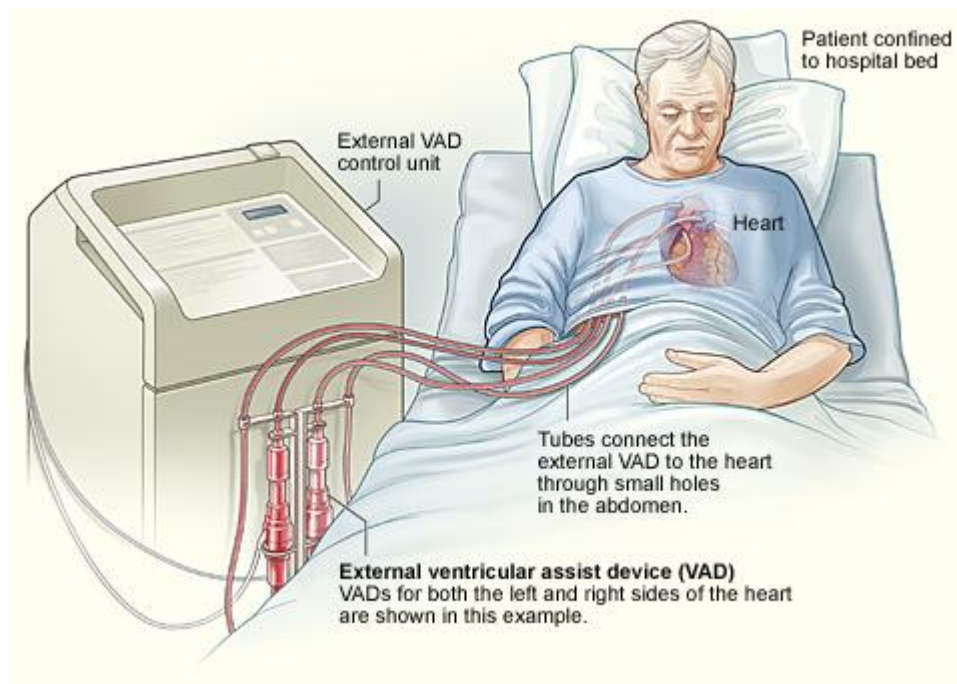
Figure 2 External VAD [25]

3.1.3   Sleep apnea treatment

Sleep apnea is a disorder, when the patient's breathing is reduced or even stopped for a short time period while asleep. So as to be recognized as an apnea, the breathing pause must be at least ten seconds long and the airflow must be lower than 25% of the normal value. Other way how to recognize an apnea is to check the blood oxygen level. If there is at least a 4% drop, we are dealing with this disorder. [26]

There are three kinds of a sleep apnea – central sleep apnea, obstructive sleep apnea and the combination of those two. The central sleep apnea is a neurological disorder, when the brain fails to properly control the breathing muscles. Then there is an obstructive sleep apnea caused by a collapse of the airway during the sleep. [27]

There are multiple ways how to treat a patient suffering from this disorder. Most complicated way is to solve this problem surgically. The treatment in this case includes a nasal surgery, tongue reduction, genioglossus advancement, maxillo-mandibular advancement, tracheostomy and others. However naturally, a surgical approach is the least desired solution. For this reason, other less invasive options are at the doctor's disposal.

If the problem does not seem to be neurological, it can be sometimes solved with a simple mouthpiece. This oral appliance may help with mild cases of the sleep apnea. It is a custom-fit plastic mouthpiece, which adjusts to a lower jaw and tongue in order to keep the airway free.
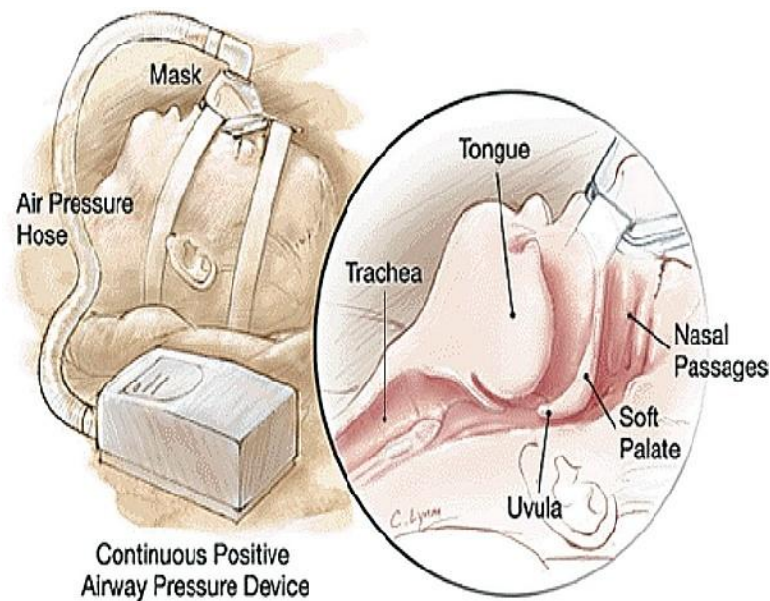

Figure 3 Continuous positive airway pressure device (CPAP) [28]

If this solution does not suffice, continuous positive airway pressure device (CPAP) is the most common treatment (Figure 3). This device is blowing an air under pressure into the throat during the sleep, so the lungs are always supplied with oxygen. The pressurized air also helps to keep the airways opened. The device is consisted of a plastic facial mask covering the patient's nose or even the mouth, which is connected to a small CPAP machine via a tube. Inside the CPAP is usually a high speed BLDC motor with an air blower. More advanced models can also monitor the patient's breathing or humidify and warm the air.[26][27]

3.1.4 Medical analyzers

Modern medicine is in large measure dependent on all sorts of chemical analysis in order to find out as much information about the patient's health as possible. The number of samples nowadays waiting to be analyzed regularly is way too large to be

dealt with by hand. For this reason, automation is being applied more and more to help improve the reliability, and speed of the analysis processes.

Figure 4 Automated benchtop blood gas analyzer [10]

The task for the BLDCs is in this case above all to very precisely manipulate with the samples between the single process steps. The samples are usually heated, cooled, and undergo other analyzation processes and it is crucial for them to be manipulated precisely and with no mistake. The manipulators also need to withstand in a close area of those processes without their behaviour to be affected. For this purpose, either a stepper motor, which is basically a subgroup of a BLDC family or a classical BLDC motor is used. Big advantage of a stepper motor is its precision caused by a high number of poled. This characteristic, however, causes lower maximum speed, which is also sometimes required for this application. It is up to the designers to decide which one of the alternative to use. [29]

3.1.5 Dental drill

A dental drill is nowadays one of the most widely used tool among dentists. So as to be able to attach a crown, bridge or dental filling, the tooth must be pre-prepared for

this procedure. That is why it has to be partially drilled and milled. Such operation is usually quite painful, because the dentist is drilling into a hard tissue. This is why it has to be as smooth as possible, which is accomplished by a high rotational speed. Together with small size, light weight and good balancing, the BLDC meets the requirements best of all alternatives.

Figure 5 Dental drill [30]

Also very similar are the drills and milling machines designed as surgical instruments. The requirements for such devices are not very different from their dental relatives. Only the range of sizes and operating power is much wider because the tools are used for multiple types of surgical performance. [31]

3.1.6 Nuclear imaging

Just like chemical analyzation, visualization of the patient's entrails is at least equally important for a right diagnose. The doctor has multiple choices in selection of the right method. There is an x-ray machine, where a 2D image in one axis is an output. Then there is a sonography – method which uses reflection of a mechanical oscillation on a high frequency, far from a hearable part of the spectrum. However, none of those uses a BLDC motor. Methods, where the BLDCs come in useful are positron emission computed tomography (ECT) or single photon emission computed tomography (SPECT). Those imaging systems use anger cameras revolving around the patient, imaging the

radiopharmaceuticals in the patient's body. The revolution is carried out by a BLDC servo, just like other motions in this system - radial movement of the cameras (because they need to be as close to the patient as possible) and horizontal movement of the patient for a full-body scan. [11]
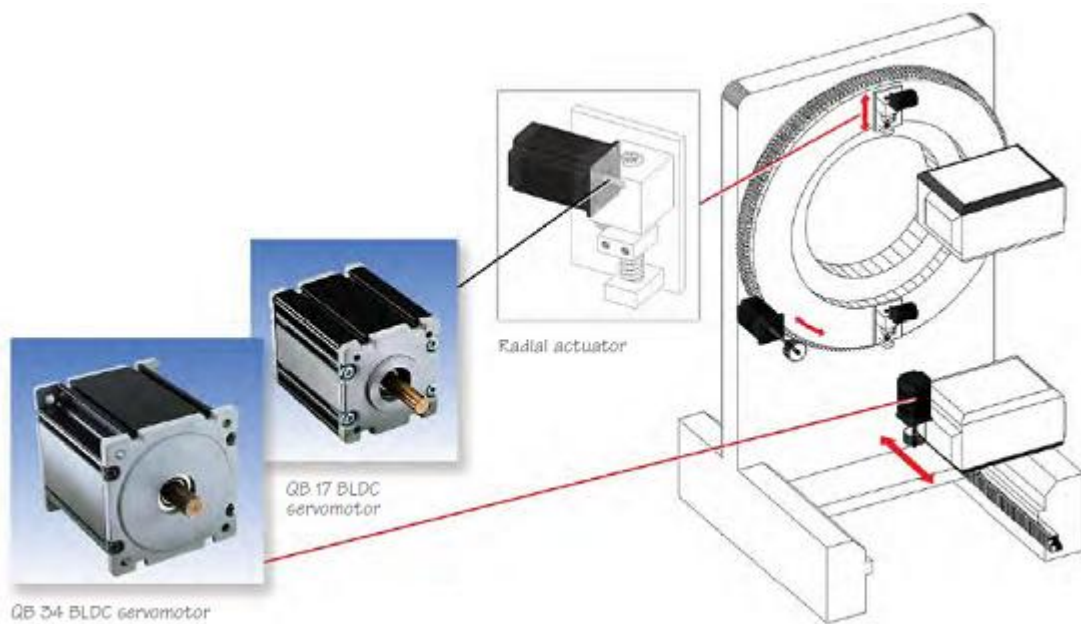

Figure 6 BLDCs in nuclear imaging [11]

3.1.7 Dialysis System

The main purpose of the kidneys is filtering waste products from the blood and regulating the body's fluid balance. Every healthy person has a pair of kidneys located on either side of the back of the abdominal cavity. If both the kidneys fail, dialysis has to take up in order to keep the blood clean. There are two kinds of dialysis – peritoneal dialysis and hemodialysis.

With peritoneal dialysis, the blood I cleaned directly in the patient's body. A catheter must be surgically placed in the abdomen. During the treatment, the dialysate flows through the catheter to the peritoneal cavity. The blood is divided from the dialysate by the peritoneum, through which the waste is drown out of the blood into the dialysate. This kind of treatment is usually prescribed to patients who are able and want to live an active life, because this way they are able to work, study or even travel. The

negatives are high requirements on the cleanness of the catheter input and the need of a big storage space for the dialysate.
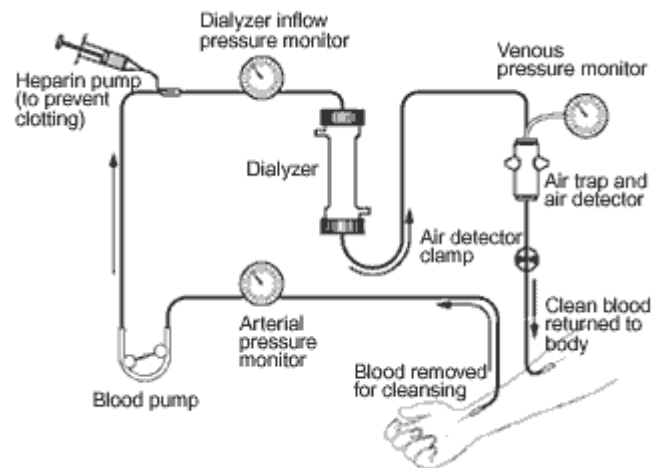

Figure 7 Hemodialysis [12]

In case the peritoneal dialysis is for some reason not suitable for the patient, hemodialysis is usually another choice. The patient has to undergo a small surgery to his arm or leg. He has a special plastic tube placed between an artery and a vein − so called gortex graft. When needed, needles are placed in the graft and the blood is lead away to the dialysis machine. There, the blood is pressed through a filter, where it leaves part of the waste, which stays in the solution on the other side of a semi-permeable membrane. There is also a venous pressure monitor, air trap and air detector in the circle, ensuring that only bubble-free blood under a correct pressure is returned to the body (Figure 7). To pump the blood through the system, a peristaltic pump is usually chosen as a solution. This is where the BLDC steps in. Although the requirements in this case are not so high (speed and torque stability, if possible low residual heat and good lifespan) the brushless motor can find its use here anyway. [12]

3.1.8   Medical mobility

An area, where the BLDCs are widely used, is medical mobility. In general, the motors here do not have to meet such high requirements like at other medical applications, the brushless DC motors however posses such advantages, that are always

welcome even at non-critical applications. Reliability, higher performance, low thermal losses and others always come in handy.

3.1.8.1 Power wheelchair

The most typical application of medical mobility is a wheelchair (Figure 8). This assistive device is crucial for people who, for various reasons, cannot walk. Simple chair on wheels has been helping the disabled partially substitute walking for centuries. Nowadays, new discoveries in the area of electrical motors and batteries allow improve this tool to be able to move on its own power so the patient does not have to use the force of his hands. Not only this is more comfortable for the disabled but it also allows the patients, who can even not move their hands, to control the chair. The battery is powerful enough to last tens of kilometers and does not need to be charged so frequently anymore. This is also caused by the lower power consumption of the BLDC. [11][22]

Figure 8 power wheelchair [13]

3.1.8.2 Wheelchair lift

Not only the patient but also his friends and family have their life complicated because of the handicap. One of the problems is transportation and handling the medical

equipment, like for example a wheelchair. Manipulation with a wheelchair can be very problematic above all for people, who are no physically very strong. At least two people are usually required to for example load the wheelchair to the car. Luckily, there are devices designed to overcome this trouble and significantly simplify the manipulation. One of those devices is a wheelchair lift equipped with motors strong enough to lift up a wheelchair, which can weight even more than 200 kg.[11]

If there is a stairway in the house, it means a great issue for the afflicted. Unfortunately, barrier-free houses are trend of the last decade or two, which means there is a big number of buildings, which are hard to access for people on a wheelchair. Good solution offers a stair lift – a device that can bring the person on the wheelchair up to a higher floor and then back down again. It is an elegant and relatively cheap solution, which can significantly help the wheelchair invalids and bring them closer to a life of a normal person. [11]

3.2 BLDC principles

This section describes the basic principles of the BLDC motor. The first part covers the problematic of the electronic commutator. Then the six-step commutation is explained. Next part of this section clarifies the way the control logic acquires the position of the rotor so as to be able to switch the phases correctly. In the end, the difference between delta and star configuration of the winding is discussed.

3.2.1 Commutator connection

As I have already implied in Chapter 1, the biggest difference between the classical DC motor and the BLDC lies in the permanent magnet of the stator at BLDC. This means that the motor cannot be commutated mechanically via the brushes, but there must be another, more sophisticated way, to do that. In case of the BLDC it is an electrical three phase inverter (Figure 9). It is consisted of six transistors, two for each phase [3].

One transistor connects the phase to the supply voltage, the second one can connect it to the ground. Third state, in which the phase can be, is when both transistors are closed and the phase is disconnected. The transistors ought to have a diode connected to their collector and emitter (or source and drain for MOSFETs) in the

reverse direction in order to protect the transistors from residual energy after disconnecting the inductive load of the winding. It is obvious that there has to be some external logic controlling the transistors. This problem is usually handled by some external logical control. It also allows us to use various algorithms dedicated to control the motor the best way possible. [22]
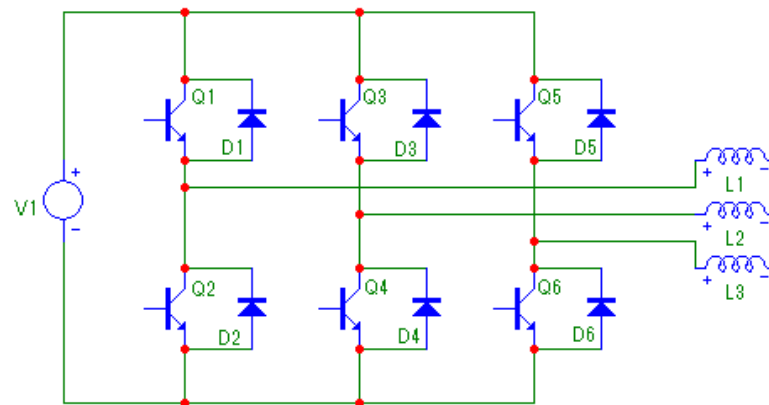

Figure 9 BLDC commutator scheme

3.2.2 Six-step control

The most common way how to control a BLDC is so called six-step control [18]. This method uses the transistors only as logical on-off switches. As the name implies, it splits the commutation phase into six logical states, which, if following each other in the right order, change the direction of the current in the winding so a proper rotational magnetic field is created. The sequence is shown in the picture 10 and table 1. The phases are in this case labeled as U, V and W.

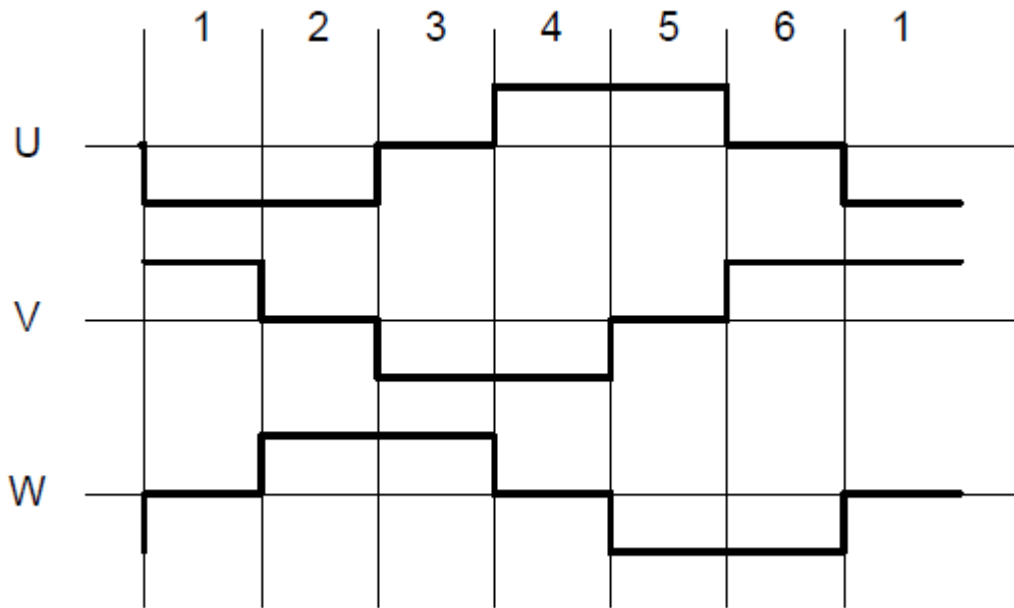|	1	2	3	4	5	6
U	-1	-1	0	1	1	0
V	1	0	-1	-1	0	1
W	0	1	1	0	-1	-1

Table 1 Six-step commutation

Figure 10 Six-step commutation [18]

If the value of the phase is 0, it means that the phase is disconnected. If it is 1, the phase is connected to the supply voltage. In case it is connected to the ground, the value in table 1 is -1. [18]

3.2.3 Position of the rotor

So as to be able to switch the transistor in the right order, the control algorithm needs to know the actual angular displacement of the rotor. There are several ways how to obtain this particular information. The most common way is to use three hall sensors, placed evenly around the rotor (with mutual angle of 120°). The sensors provide real-time discrete information about the magnetic field in their surroundings, which is closely related to the rotor's position. This kind of control is very comfortable for the developers but it is more expensive in a series production. Cheaper way is to leave out the sensors and use a sensorless method. With this method, the control unit does not read any output of sensors, but measures a so called Back EMF, which is a voltage occurring on the winding. This is caused by the winding's wires cutting the magnetic field. According to

the Farady's law of induction, the motor acts like a generator and a voltage proportional to the speed of the rotor emerges on the phases. By the Lenz's law this voltage opposes the original voltage on the coil. Knowing this phenomenon, we are then able to read a voltage drop on each phase and therefore calculate an actual angular displacement of the rotor [3][22].

3.2.4 Connection of the phases

There are two ways how to connect a three-phase winding – star connection (Y) and delta connection (Δ) (Figure 11). In general, delta connection is not used very often because of the circulation current caused by the triple harmonics [2]. However, this problem can be solved via precise construction of the motor and right choice of number of poles and slots [2].
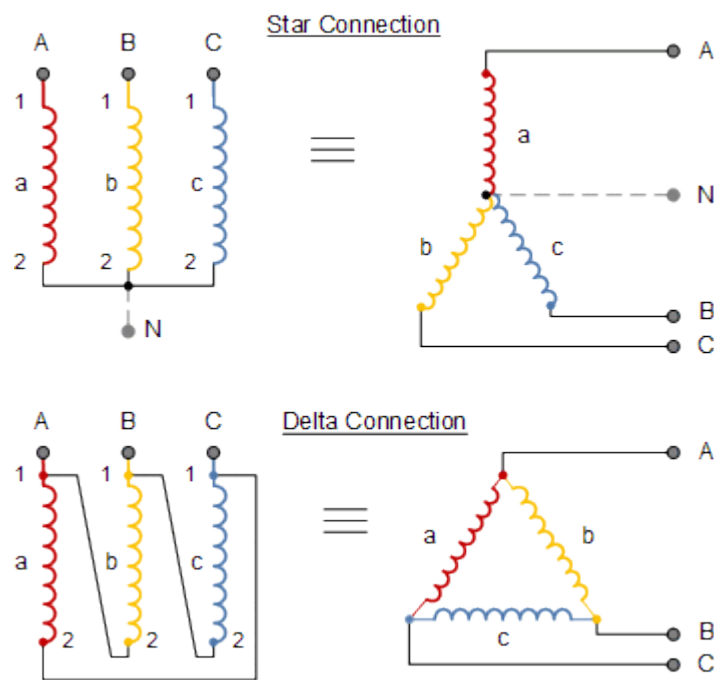
Figure 11 Star and Delta configurations [19]

Unlike the star winding delta winding is also easier and cheaper to manufacture, which makes it more suitable for mass production. Considering the power consumption of the motor, star winding has better parameters, which also corresponds with lower

mechanical power of the shaft. Parameter comparison of both configurations is in the Table 2 [2].

	Manufacturing price	Power consumption	Mechanical power	Circulation current
Star winding	Higher	Lower	Lower	No
Delta winding	Lower	Higher	higher	Yes

Table 2 Star and Delta winding comparison

3.3 Simulation possibilities for DC and BLDC motors

One of the goals of this thesis is to create a software model of the BLDC motor. For this task it is necessary to choose a proper tool on which the model would be designed.

3.3.1 Simulation requirements

Classical DC motor is one of the most typical systems used as a simulation example. If the commutation influence and other non-linearities are neglected, the DC motor can be described only with a few equations. This simplification allows us to define the output torque as a function of input current and the angular velocity as a function of input voltage [20]. Model like that can be described with most of the modern simulation tools. The BLDC motor, however, must be simulated in a more complicated way. Since the commutator does not use the brushes, where their influence can be compensated via a constant, the commutation itself must be at least partially simulated. This brings a significant non-linearity to the model, which has to be somehow dealt with [1].

3.3.2 Matlab Simulink

Matlab Simulink is today's one of the most proven numerical simulation software created by the Mathworks company. It works with a network of mutually connected blocks that process the signals flowing from one to another (causal data flow graphical programming). Each block has one or more inputs and outputs. Simulink offers a library with a great amount of basic blocks like multipliers, dividers, integrators, adders and so

on, that allows us to put together basically any kind of a dynamic system. It is also possible to insert parts of the system into subsystems, which enables to make the final model more transparent. The user can also write his own blocks in the programming language C. Important fact is, that the resulting network is not a graphical expression of the equations but more of a visual representation of the calculation procedure. [16] It is possible to extend the Simulink environment with additional add-on products. In case of modeling the BLDC motors for medical applications, SimElectronics, SimPowerSystems or Simscape might be useful. SimElectronics allows the user to add components like semiconductors, drives, sensors actuators and others. SimPowerSystems provides libraries related to electrical power systems. For example three-phase machines, electric drives or AC transmission systems can be simulated with this library. Simscape is used for acausal simulating in an amount of physical domains. Libraries for mechanical, electrical, hydraulical or other domains are at the user's disposal. However, although those additional libraries can significantly simplify the work and lower the effort which has to be spend on the simulation, most of the systems can be created using only Matlab Simulink [34].

3.3.3 Modelica

Another approach to dynamic system modeling is so called acausal modeling. In this case, the model is considered as a system of equations and not as a calculation procedure. The system can be divided into blocks but here, every block is defined by the equations. Those equations, however, do not assign values to variables but express the relations between variables as a complex system – just the way the physicists describe it [16]. This way is called declarative description of the algorithm because it approaches the system as a complex. Advantage of this method is that it is easier to find a mistake. For example the number of equations and variable has to always match. Otherwise, the model would be overdeclared or underdeclared and impossible to solve [16][35]. The blocks are connected together via connectors. Modelica introduces us an important type of connector – flow connector. Over this connector, flow variables like fluid flow or electrical current are connected. Owing to this, the system has to follow rules similar to the Kirchhoff's circuit laws because the algebraic sum of flow variables meeting at a point is zero and sum of potential differences equals the total potential difference in the

loop. This way Modelica prevents more possible mistakes in the model. The Modelica language was originally written in Sweden and it is developed as a free-ware distribution or as a commercial product (Dymola by Dynasim - Dassault Systems and MathModelica by Math-Core) [16][35].

3.3.4 NI electric motor simulation toolkit

A completely different approach was chosen by the company National Instruments. Their idea was to use their software environment combined with NI analog input/output card to completely simulate the electrical signals coming in and out of the motor. In order to create as accurate model as possible, they have combined the finite-element analysis (FEA) with the classical description of the model with a set of differential equations.
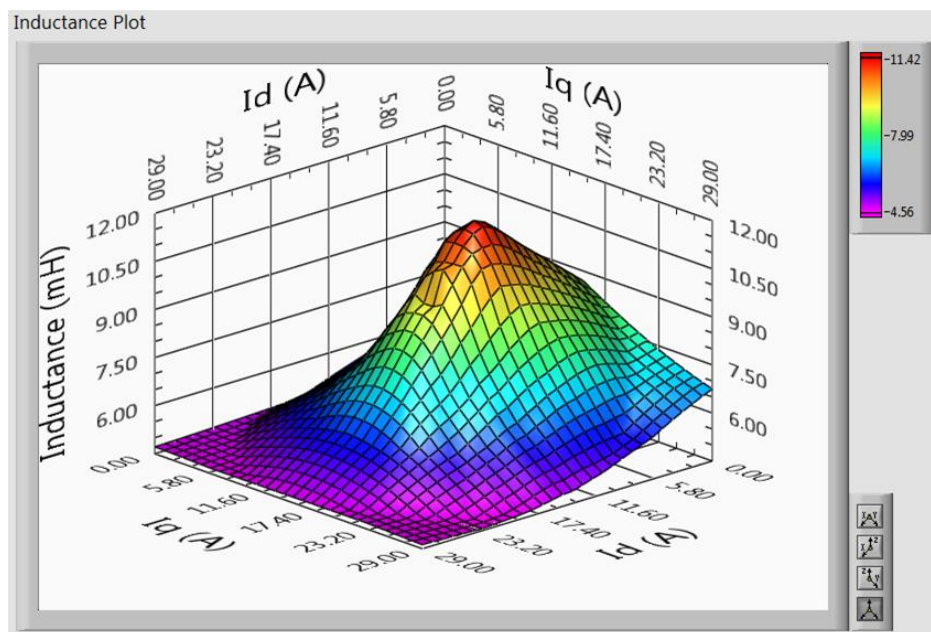
Figure 12 Lookup table for inductance variations [17]

First step is to simulate the motor with the finite element analysis (FEA). This means that a 3D model of the motor in a JMAG development environment must be created. On this model, all possible non-linearities (such as cogging torque or magnetic saturation) are simulated. This allows us to generate a lookup table capturing a complex behavior of the motor without modeling it directly in the simulation (Figure 12). Of

course, this part is created "offline" and the calculation of the lookup table takes a great deal of time. The next step is creating a complex mathematical model of the motor. This model is then used for a real-time calculation of the motor's state space with help of the lookup table [17].

An issue is presented by the real-time calculation speed. Although the lookup table decreases the calculation time of each simulation step significantly, an ordinary PC cannot compute it fast enough anyway. For this reason, NI provides a Xilinx FPGA card which allows them to compress the simulation step down to 1 μS. This corresponds with the frequency of 1 MHz, which is a sufficient speed for an effective simulation [17].

This whole solution is put into practice via the NI Veristand software. This environment is in general designed for a real-time target-to-host communication, data logging, stimulus generation and others. It allows a so called hardware in the loop (HIL) testing on the model, created by the user [17].

3.3.5   Comparison of the simulation tools

It is hard to tell which one of the simulation tools is the best because each one of them has its advantages and disadvantages. It is up to the user to decide, which approach suits him the most and which way is better for the given application. In Table 3, I have tried to compare the tools using some criteria, I have found important. Nevertheless, it is necessary to say that this comparison is strictly my personal opinion.

Simulation Tool	Fidelity of the model	Principle of the model	Availability of the model	Computational Complexity	Configurability of the parameters
Modelica	Good	Acausal	Good	Low	Good
NI HIL toolkit	Very Good	Combination of both	Currently developed	Real-Time	Very Good
Matlab Simulink	Good	Causal	Best	High	Good

Table 3 Comparison of the simulation tools

4 Software model of the BLDC

This chapter is about the software model of the BLDC. At first it was necessary to create a mathematical description of the model. I am describing both, the star winding model and delta winding model. Next step is defining the values of the constants in the equations. The way the parameters have been measured is clarified in Chapter 4.2. Apart from the usual constants, also the behavior of the measured Back EMF is described in this chapter. With the proper equations and constants, I am then able to design a Simulink model for star and delta winding. Description of the model and its evaluation are in Chapter 4.3.

4.1 Mathematical model of the BLDC

As mentioned above, I have described both star and delta winding. The mathematical description is divided into two parts: electrical and mechanical equations.

4.1.1 Star-winding BLDC motor

4.1.1.1 Electrical equations

For each phase, the following equation is defined [1]:

$$u_a(t) = i_a(t)R_a + L_a \frac{di_a(t)}{dt} + e_a(t) \tag{1}$$

$$u_b(t) = i_b(t)R_b + L_b \frac{di_b(t)}{dt} + e_b(t) \tag{2}$$

$$u_c(t) = i_c(t)R_c + L_c \frac{di_c(t)}{dt} + e_c(t) \tag{3}$$

Where
- u [V] is voltage on each phase
- i [A] is current in the phase
- R [Ohm] is resistance of the phase
- L [H] is inductance of the phase
- e [V] is a Back-EMF

4.1.1.2 Mechanical equations

$$T_{elmag}(t) = \omega(t)b + J\frac{d\omega(t)}{dt} + T_{load}(t) \tag{4}$$

Where
- T_{elmag}[N.m] is an electromagnetic torque
- T_{load} [N.m] is a load torque
- ω [rad/s] is an angular speed
- J [kg.m²] rotor's moment of inertia
- b [N.m.s] is a viscous friction constant

The Torque of one phase can be expressed with an equation [1]:

$$T_a(t) = \frac{P_a(t)}{\omega(t)} = \frac{i_a(t)e_a(t)}{\omega(t)} \tag{5}$$

For all three phases combined, the equation is [1]:

$$T(t) = \frac{P(t)}{\omega(t)} = \frac{i_a(t)e_a(t)+i_b(t)e_b(t)+i_c(t)e_c(t)}{\omega(t)} \tag{6}$$

Where
- T_a[N.m] is a torque of one phase
- P_a[W] is a power of one phase
- P[W] is a power of all phases
- $e_{a,b,c}$[V] is a Back-EMF
- ω[rad/s] is an angular speed

Every BLDC motor can have one or more pole-pairs. The relation between the number of pole-pairs, angular speed and angular displacement is expressed by equation (7) [1].

$$\omega(t) = \frac{2}{Pp}\frac{d\varphi(t)}{dt} \tag{7}$$

Where   - ω[rad/s] is an angular speed

                                       - φ [rad] is angular displacement

                                       - Pp [-] is number of pole-pairs

4.1.2   Delta connected BLDC motor

The BLDC is usually connected as a star. Sometimes, however, the winding is connected as a delta. The main reason, why this is used is because the delta winding is easier to manufacture [2].
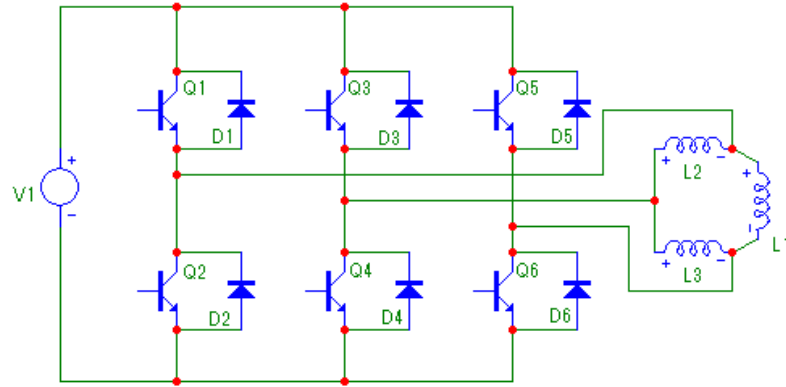
Figure 13 Delta connected BLDC

The electrical equation is logically changed a little. One clamp is connected to the supply voltage, second clamp is connected to the ground and third clamp is disconnected. All three phases then make a serio-parallel connection. One coil in one branch and two coils in series in the second branch. The impedance of the whole system is smaller than in the first case, which means the motor has a bigger power in this connection [2].

$$u_{dc}(t) = i_c(t)R_c + L_c \frac{di_c(t)}{dt} + e_c(t) \tag{8}$$

$$u_{dc}(t) = i_a(t)R_a + L_a \frac{di_a(t)}{dt} - e_a(t) + i_b(t)R_b + L_b \frac{di_b(t)}{dt} - e_b(t) \tag{9}$$

$$e_a + e_b + e_b = 0 \tag{10}$$

24

Where   - u_{dc} [V] is a supply voltage

$\text{- } i_{a,b,c}$ [A] is current in the phase

$\text{- } R_{a,b,c}$ [Ohm] is resistance of the phase

$\text{- } L_{a,b,c}$ [H] is inductance of the phase

$\text{- } e_{a,b,c}$ [V] is a Back-EMF on the phase

In this case, it makes more sense to express equation for the supply voltage. Phase A and B are connected in a series. Phase C is connected parallel to A and B. Because the sum of the back-EMF induced on all phases is zero (10), the back-EMF must be subtracted in equation (9). Voltage between the phase A and B is expressed by equation (11) [2].

$$u_{ab} = \frac{1}{2}u_{dc} + \frac{1}{2}e_c + e_a \tag{11}$$

Where $\text{- } u_{dc}$ [V] is a supply voltage

$\text{- } u_{ab}$ [V] is a voltage on one phase

$\text{- } e_{a,b,c}$ [V] is a Back-EMF on the phase

4.2 Parameters identification

In order to make the model act like a real pump, I had to correctly measure its parameters. Since our information about the motor are rather limited I had to come up or find proper measuring methods in literature so as to obtain their values [32]. For the sake of simplicity, I assume that all three phases are identical in every way. The constants I have measured and their values are in the Table 4.

Parameter	Value
Phase resistance R [Ohm]	0,125
Phase inductance L [mH]	0,163
Moment of inertia J [g.cm^2]	19,9
Electrical constant e [V/rad]	0,02
Back EMF power constant Pe [W/rad]	0,003
Number of pole-pairs Pp [-]	4
Viscouse friction b [N.m.s]	0,0008

Table 4 Measured constants overview

4.2.1 Phase resistance

This parameter is the first that needed to be measured. Each phase is a coil, which acts like a short-circuit when supplied with a direct current. The only condition is to measure long enough after the transient response of the winding. After the circuit reaches its equilibrium again, we measure a piece of wire in the ohmmeter's point of view. This means the phase resistance should be very small. There is a difference between the star winding and delta winding. In case the winding is a star, the phase resistance is rather simple

$$R_{phase} = R_{measured}/2 \tag{12}$$

Where   - R_{phase} [Ohm] is resistance of one phase

                            - $R_{measured}$ [Ohm] is the measured resistance

For the delta winding, the phase resistance is a little bit more difficult to calculate. The Resistance between two phases is

$$R = \frac{(R_1+R_2)R_3}{R_1+R_2+R_3} = \frac{2R_{phase}^2}{3R_{phase}} = \frac{2}{3}R_{phase} \tag{13}$$

Where $R_1 + R_2 + R_3 = R_{phase}$ are the resistances of each phase. Therefore

$$R_{phase} = \frac{3}{2}R \tag{14}$$

I have measured the resistance with an OM21 micro-ohmmeter with accuracy of 0.03% [4]. The measured resistance between two phases is 187 mΩ (range 200 mΩ, measurement current 100mA). Using (13), the resistance of one phase is 125 mΩ. According to the datasheet, the resistance of one phase should be smaller than 170mΩ [32]. We can say that the measured value corresponds with the value defined in the datasheet. I have decided to use the value I have measured for the simulation.

4.2.2 Phase inductance

There are two kinds of inductances, when we talk about the BLDC – direct inductance and quadrature inductance and their values correspond to the rotor position [36]. Those inductances are in general different, but for the sake of simplicity, I have neglected their difference and measured the inductance as one parameter $L = L_d = L_q$. Since the inductance is quite important aspect of the system, I have performed two methods of measurement – by measuring the frequency response of the winding and by using a professional RLC meter.

4.2.2.1 Frequency response measurement

The idea of this measurement is to supply the winding with an alternating voltage, while measuring the input current. The impedance of a coil is defined

$$Z = \sqrt{R^2 + X_L^2} = \sqrt{R^2 + L^2 \omega^2} \tag{15}$$

where R is the phase resistance, which we have already defined and X_L^2 is inductive reactance of the coil. Omega is in this case an angular velocity, which is derived from the frequency of the supply voltage

$$\omega = 2\pi f \tag{16}$$

Now we can express the inductance

$$L = \frac{1}{\omega} \sqrt{Z^2 - R^2} \tag{17}$$

Considering

$$Z = \frac{U}{I} \tag{18}$$

Where U and I are effective values of the input current and voltage, we can express the inductance

$$L = \frac{1}{\omega} \sqrt{\frac{U^2}{I^2} - R^2} \qquad (19)$$

Since the phase resistance is very low, I needed to use a power source able to supply the circuit with a high current on a frequency 1 kHz and higher. For this purpose I was unable to use a standard function generator, because it cannot generate high power signals. For this reason I have used a high-frequency tone generator, designed for ultrasonic welding machine calibration. It is basically an amplifier for acoustic signals, which can work on ultrasound frequencies (in this case up to 35 kHz). The input signal was a standard low power sinus function, which was then amplified to a high power 1V RMS. The output power signal was connected directly to the winding.
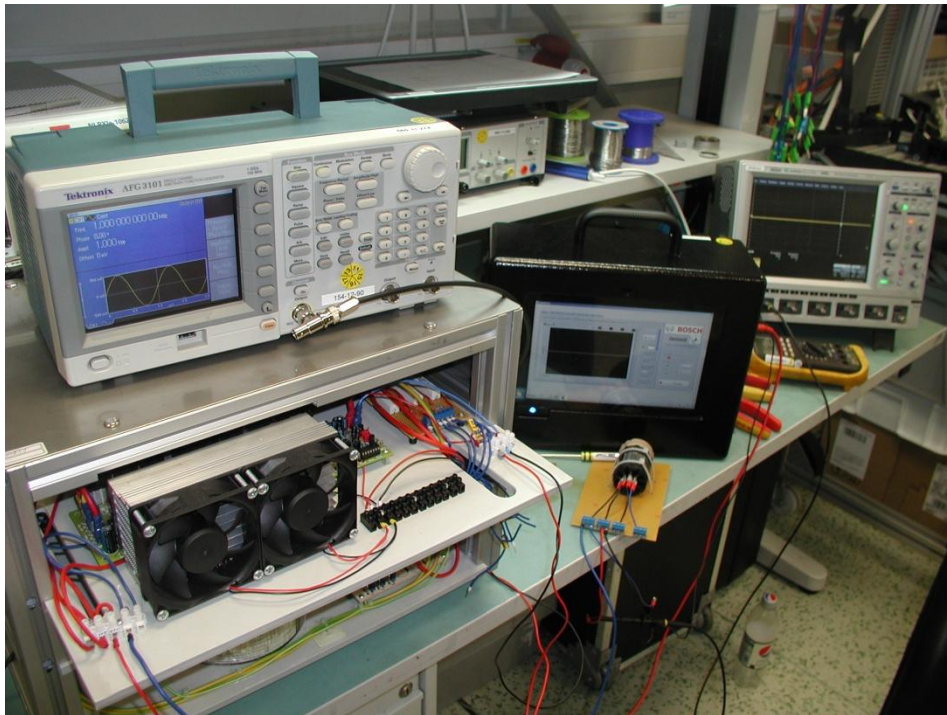
Figure 14 Inductance measurement setup

I was measuring the voltage, its frequency and input current. The frequency range was 1-5 kHz. I have measured the values for five frequencies and calculated the

inductance for each frequency using (19). The resulting frequency was then a mean of those values. To calculate the inductance of one phase, I have used the same procedure like for the resistance. The inductance of one phase is then expressed

$$L = \frac{(L_1+L_2)L_3}{L_1+L_2+L_3} = \frac{2L_{phase}^2}{3L_{phase}} = \frac{2}{3}L_{phase} \tag{20}$$

$$L_{phase} = \frac{3}{2}L \tag{21}$$

With this approach, the resulting inductance of one phase was 0,163 mH. I have used this value for my simulation.
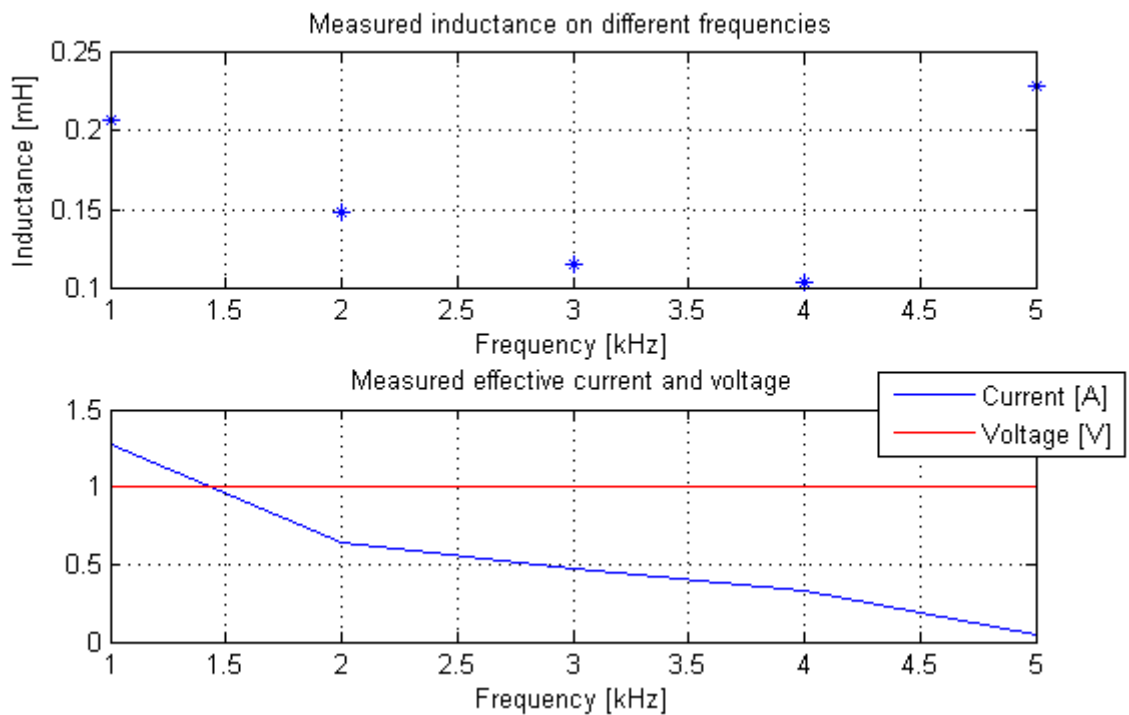
Figure 15 Results of the inductance measurement

4.2.2.2   RLC meter measurement

As a second way I have used FLUKE PM6306 RLC meter to measure the phase inductance. In order to unify the measurement, I have set the input frequency to 1 kHz. However, because the RLC meter sets the voltage automatically, the input voltage was 9,45 mV and the current 9,97 mA. With this configuration I have measured the serio-parallel inductance 0,1162 mH (0,1% basic accuracy declared by the manufacturer [5]), which according to (20) and (21) means the phase inductance of 0,1743 mH. The device also indicates the phase shift, which in this case was φ = 74°. The difference between this measurement and the previous one is 11 µH.

4.2.3   Moment of Inertia

The rotor's inertia is one of the few parameters, which were provided by the manufacturer. Its value is 19,9 g.cm^2 [32].

4.2.4   Back-EMF

As mentioned before, the movement of the rotor creates a voltage on the winding with amplitude proportional to the angular speed. The frequency of the back-EMF corresponds to the angular speed and also to the number of pole-pairs. This voltage is not constant, but has a form of a trapezoid, above all by low rotational speed. The trapezoidal function is defined [1]:

$$
f(\Theta) = \begin{cases}
\left(\dfrac{6}{\pi}\right)\Theta & \left(0 < \Theta < \dfrac{\pi}{6}\right) \\[2mm]
1 & \left(\dfrac{\pi}{6} < \Theta < \dfrac{5\pi}{6}\right) \\[2mm]
-\left(\dfrac{6}{\pi}\right)\Theta & \left(\dfrac{5\pi}{6} < \Theta < \dfrac{7\pi}{6}\right) \\[2mm]
-1 & \left(\dfrac{7\pi}{6} < \Theta < \dfrac{11\pi}{6}\right) \\[2mm]
\left(\dfrac{6}{\pi}\right)\Theta - 12 & \left(\dfrac{11\pi}{6} < \Theta < 2\pi\right)
\end{cases}
$$

The phase difference between the phases is $\frac{2}{3}\pi$.

4.2.4.1 Measurement of the Back-EMF

For a valid simulation, the Back-EMF behavior needed to be measured. Therefore, I have performed a test to simulate spinning of the rotor, while measuring the induced voltage of each phase. To do so, I have disconnected the measured motor from the supply voltage and welded its spindle to another BLDC's shaft. This way I was able to spin the rotor without the supply voltage and measure only the Back-EMF on its clamps.

Figure 16 Back-EMF measurement

4.2.4.2 Measurement of the Back-EMF without load

I have performed the first measurement without any load. Since I did not know the number of pole-pairs, I was not able to determine the angular speed by the EMF frequency. For this reason, I used a digital non contact photo laser tachometer. This method uses a reflective sticker placed on the spindle. The tachometer then radiates a laser beam, which is reflected with a period proportional to the angular speed of the rotor.

As displayed in the figure 17, the Back-EMF really has a trapezoidal character on low frequency. However, on high speed, the function gets more of a sinusoidal character (Figure 18).
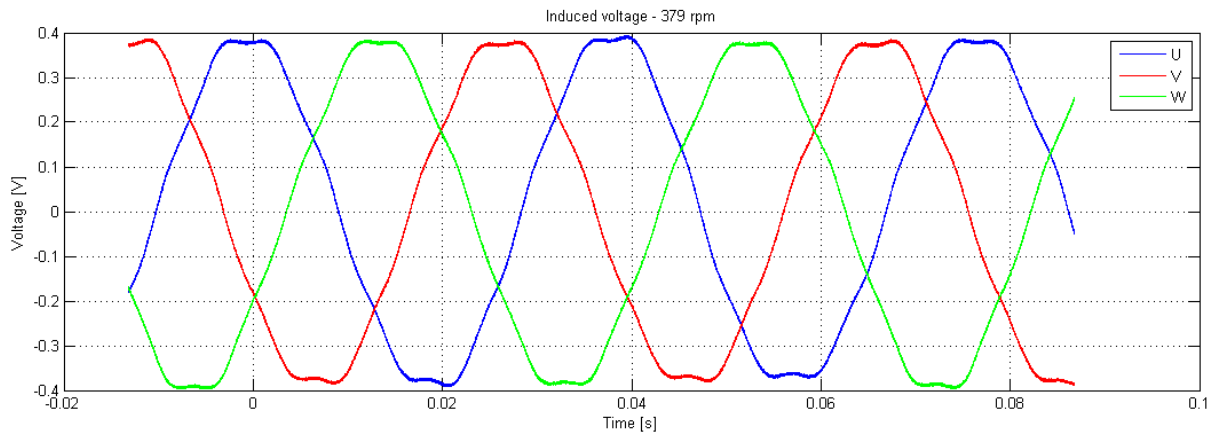
Figure 17 The low-speed Back-EMF
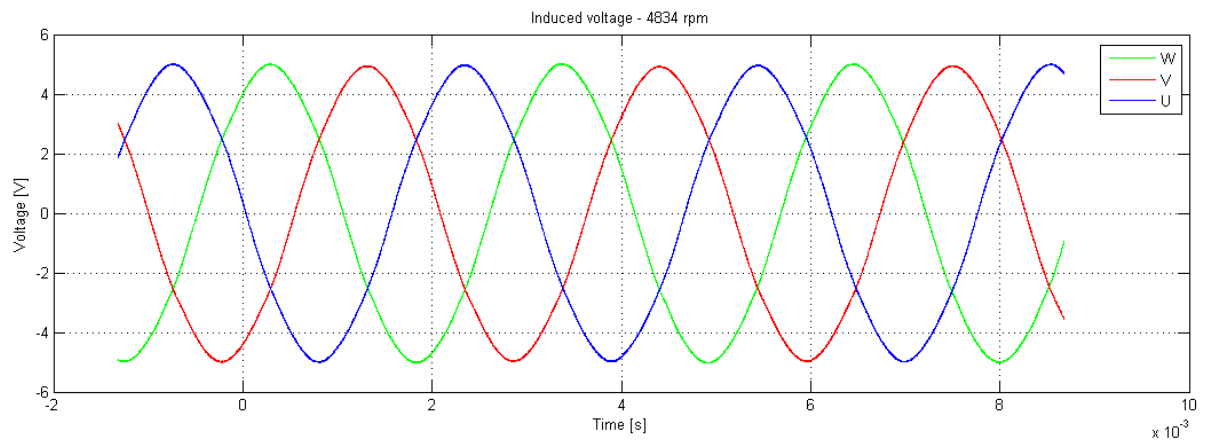
Figure 18 The high-speed Back-EMF

Another parameter I was interested in is the dependency of the amplitude on the angular speed. As shown in the Figure 19, the relation is perfectly linear on the measured speed range. At this point, we can define a constant determining the slope of this function – an electrical constant. In this case, it is e = 0,02 V.s/rad.
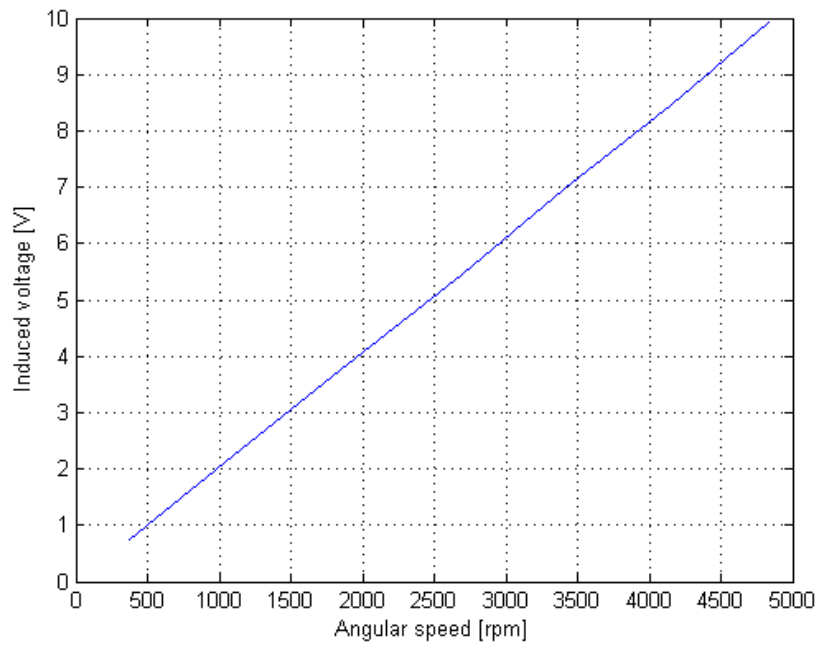
Figure 19 Relation between angular speed and induced voltage

4.2.4.3 Measurement of the Back-EMF with load

To measure the back-EMF with load, I have connected three 10Ω resistors as a star, each of its ends to one phase. Their common center was connected to the ground and worked as a negative pole for the voltage measurement.
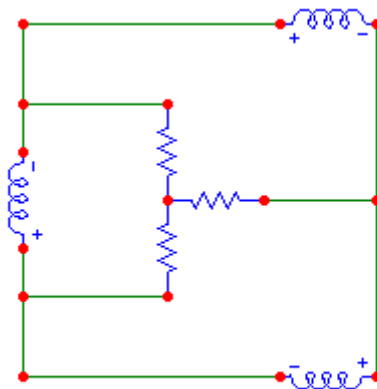
Figure 20 Back-EMF with load measurement
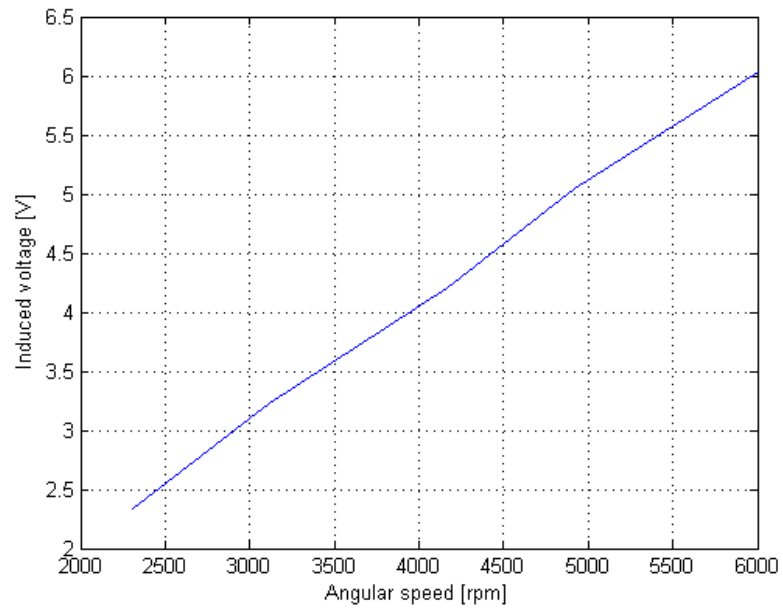
Figure 21 Back EMF amplitude with load

The relation between angular speed and induced voltage is also linear like in the first case, only this time the slope is smaller. Since I had induced voltage and resistance, I was able to calculate an electrical power of the back EMF using the formula $P = \frac{U^2}{R}$. The result is in the Figure 22.
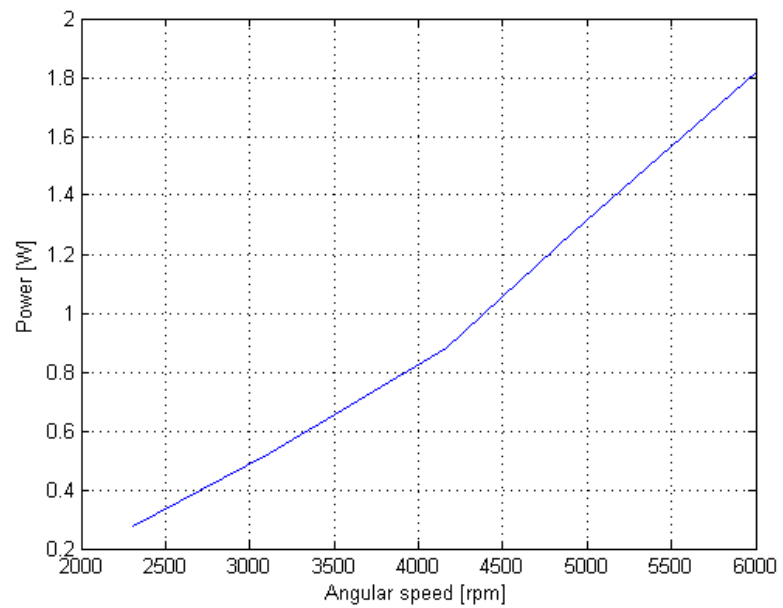
Figure 22 Back EMF power

The electrical constant is now e = 0,01 V.s/rad. We can also define a power constant of the back EMF, which is Pe = 0,003W.s/rad.

4.2.5 Number of pole-pairs

The number of pole-pairs is quite easy to calculate. From the Back EMF measurement, I knew the frequency of the generated electromagnetic field and the speed of the shaft (Chapter 4.2.4.2). Using the formula

$$Number\ of\ pole\ pairs = \frac{60\ f}{\omega} = \frac{60 * 332}{4834} \approx 4 \qquad (22)$$

Where
- f [Hz] is the switching frequency of one phase
- ω[rad/s] is an angular speed of the shaft

The number of pole pairs is four.

4.2.6 Viscous friction

I have obtained the viscous friction parameter from the model itself. Since it was the only parameter left, I have adjusted it so the model was as close to the real motor as possible. The value of this constant is b = 0,0008 N.m.s

4.3 Simulation of the BLDC in Matlab Simulink

I have performed a simulation of two systems: a BLDC motor with a star winding and a BLDC motor with a delta winding. Star winding was simulated because it is a typical way of manufacturing the motor. Delta winding is less common, it is however installed to the products that our company produces and therefore I am working with it in my thesis.

4.3.1 Star winding model

The model is consisted of two files. A Matlab script, which defines all the necessary variables, then calls the model and plots the results. Second file is and .slx file with the actual model. The model contains four main blocks representing the equations

of the mathematical model. First block calculates the current of all three phases out of the supply voltage and the back-EMF (Figure 23).
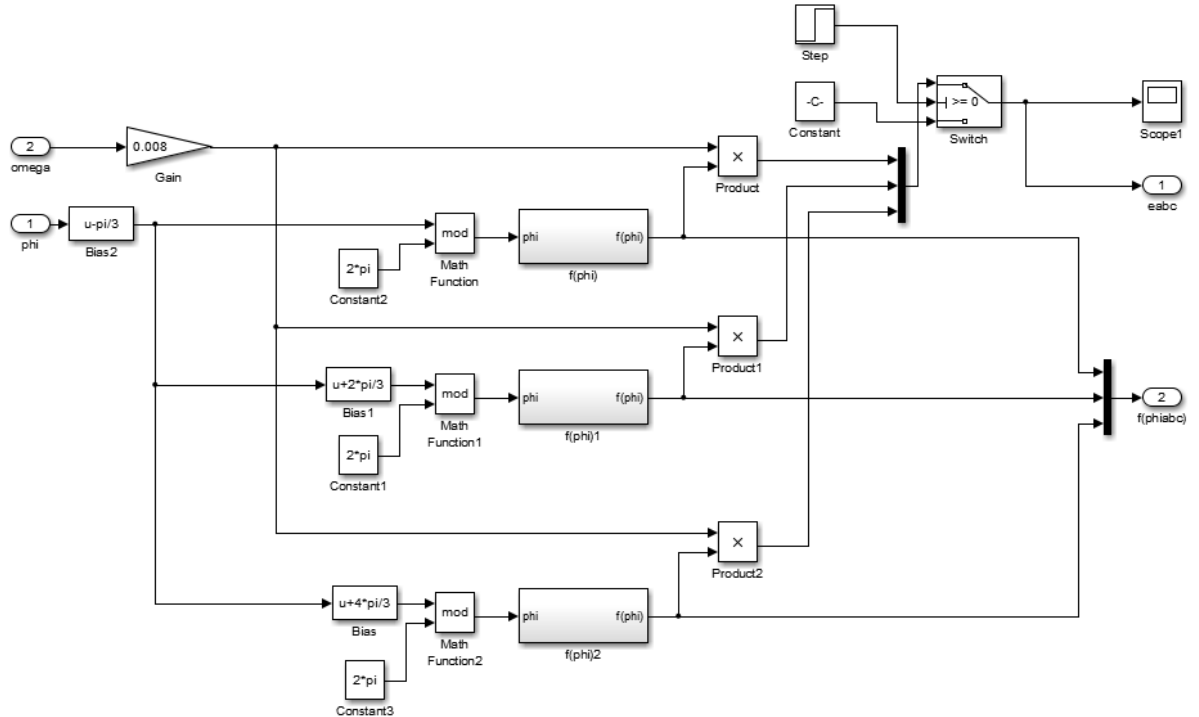

Figure 23 Simulink Back EMF generation block

Second block expresses the electromagnetic torque using the currents vector, angular speed, and back-EMF as an input. Third block generates angular displacement and angular speed from total torque of the machine, which is acquired by subtracting torque of the load from the electrical torque. Last block calculates the Back-EMF from the angular speed and displacement. The main schema of the mode is shown in the picture 24.
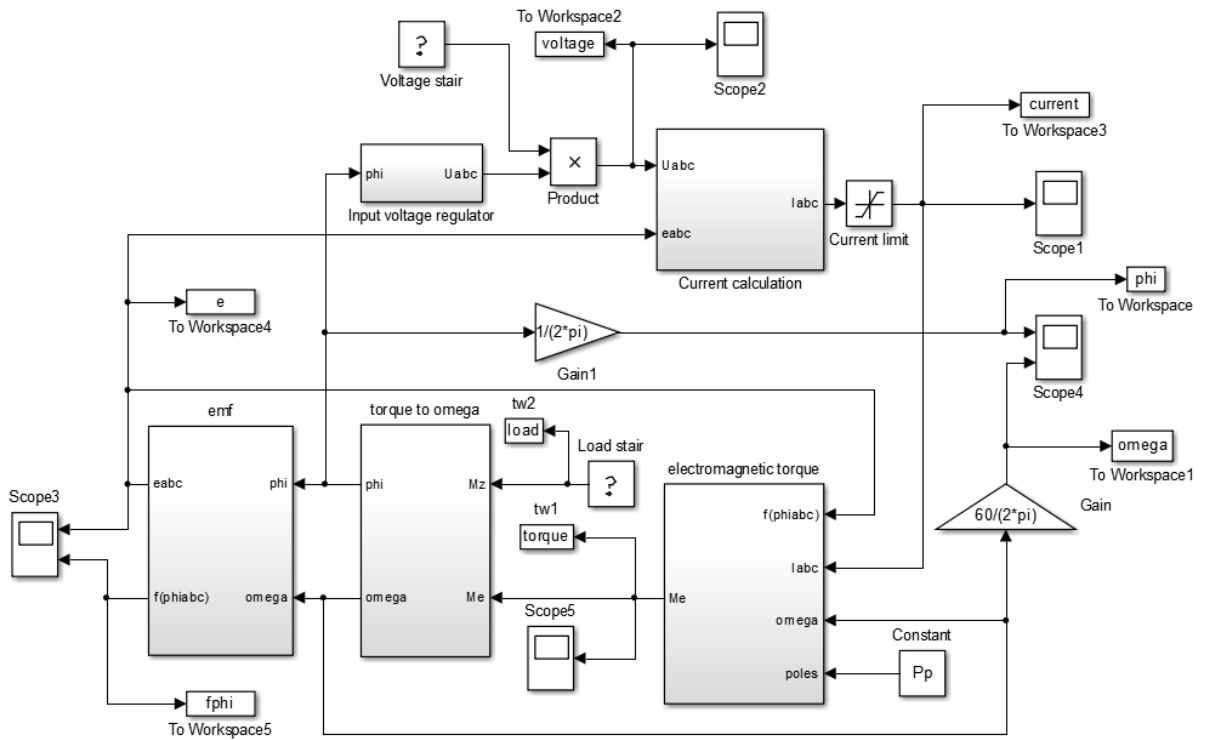
Figure 24 Schema of the BLDC model in Matlab Simulink

The model also contains an input voltage regulator. This is a submodel of the BLDC commutator, which controls the input voltage of all three phases (Figure 25).
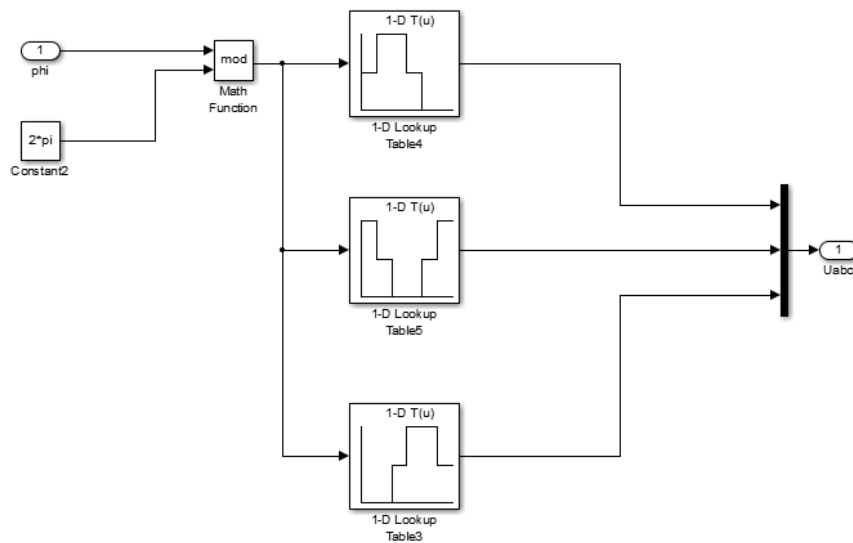
Figure 25 Simulink BLDC commutator

It is necessary to say that the commutator is a simple function generating the phase voltage signals based on the angular displacement. In general the commutator is not a part of the BLDC motor. It however affects the behavior of the motor greatly and the motor cannot be simulated without it.
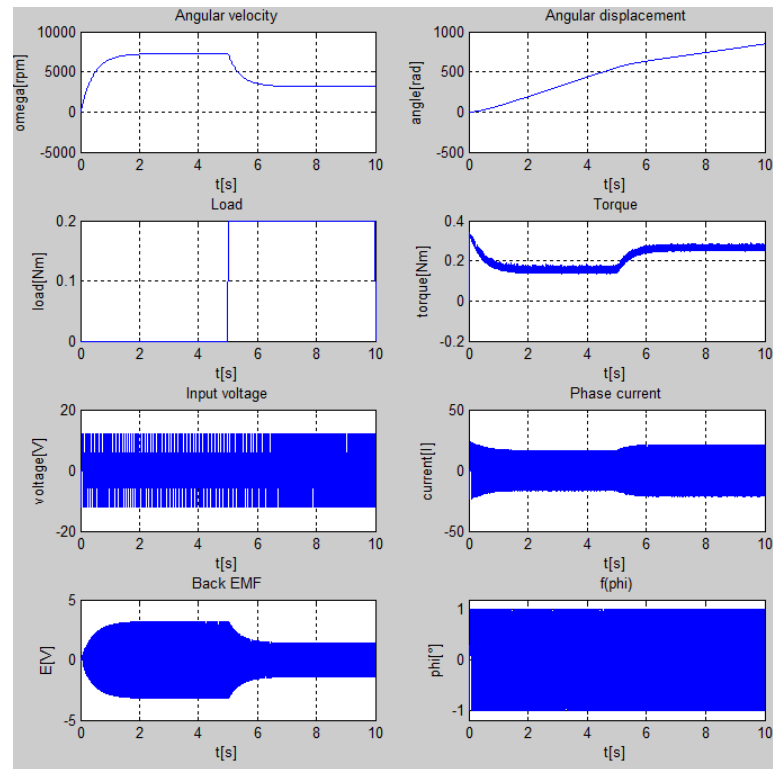
Figure 26 Output of the model

As you can see in the Figure 26, the graphical interface of the star winding model shows all the outputs of the model: angular velocity, angular displacement, load, torque, supply voltage for the phases, phase current, Back-EMF and the trapezoidal function. In this case, there is a change of load in time 5s to 0.2 Nm so as to show the influence of the load on the angular velocity, torque and other parameters.

4.3.2 Delta winding model

The delta winding model is similar to the star winding model. The current calculation block has been changed according to equations (8), (9), (10) and (11). The block is in this case a little bit more complex because the transfer function of the

winding is not just two inductances connected in parallel but a serio-parallel combination.

4.3.3 Model evaluation

I have measured the starting time of the motor. Because I needed this piece of data as precise as possible, I have used an oscilloscope to measure the switching period of the control unit from time zero to the time of full speed and then recalculated it to an angular velocity. After acquiring the data, I was then able to compare the real behaviour of the motor with both of the models.
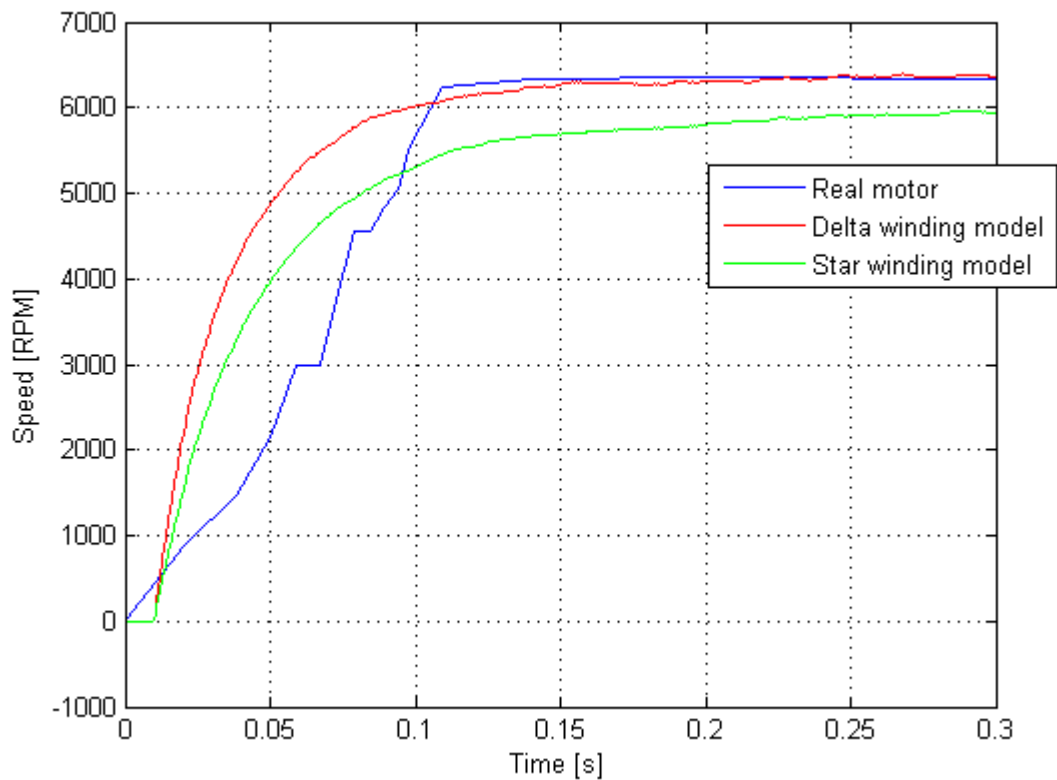
Figure 27 Starting time comparison

According to Figure 27, the final speed of the motor and the delta winding model is approximately comparable. Final speed of the star winding model is lower, which matches the assumption, because the energy consumption of the star is lower. The rising edge of the models is more fluent, which is caused by the measurement method I have used for obtaining the speed waveform.
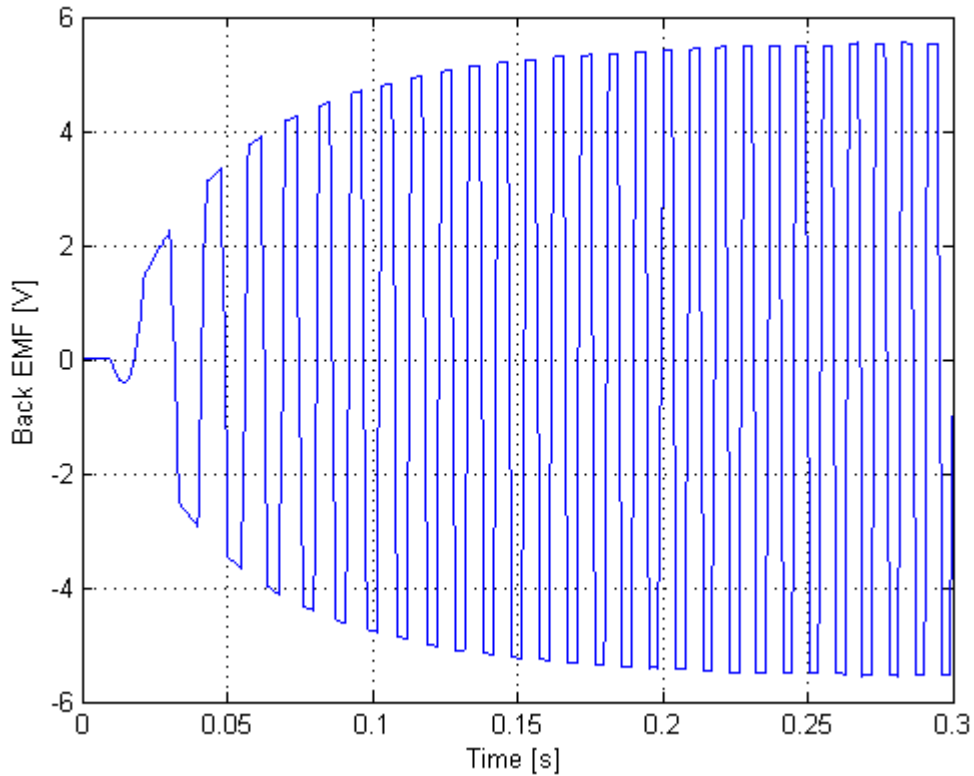
Figure 28 Back EMF of the model

In the picture 28, there is simulated shape of the Back EMF curve of the star model. Unlike the real behaviour from the Back EMF measurement, the model holds the trapezoidal form even on higher angular velocity. The EMF function is simplified and the sinusoidal character of the curve on high speed has been neglected. I do not, however, believe that it could significantly influence the fidelity of the simulation.

Figure 29 shows us the relationship between the angular velocity and angular displacement. The angular displacement in this case directly depends on the angular velocity. It is obtained by integrating the omega value over the measured time period.
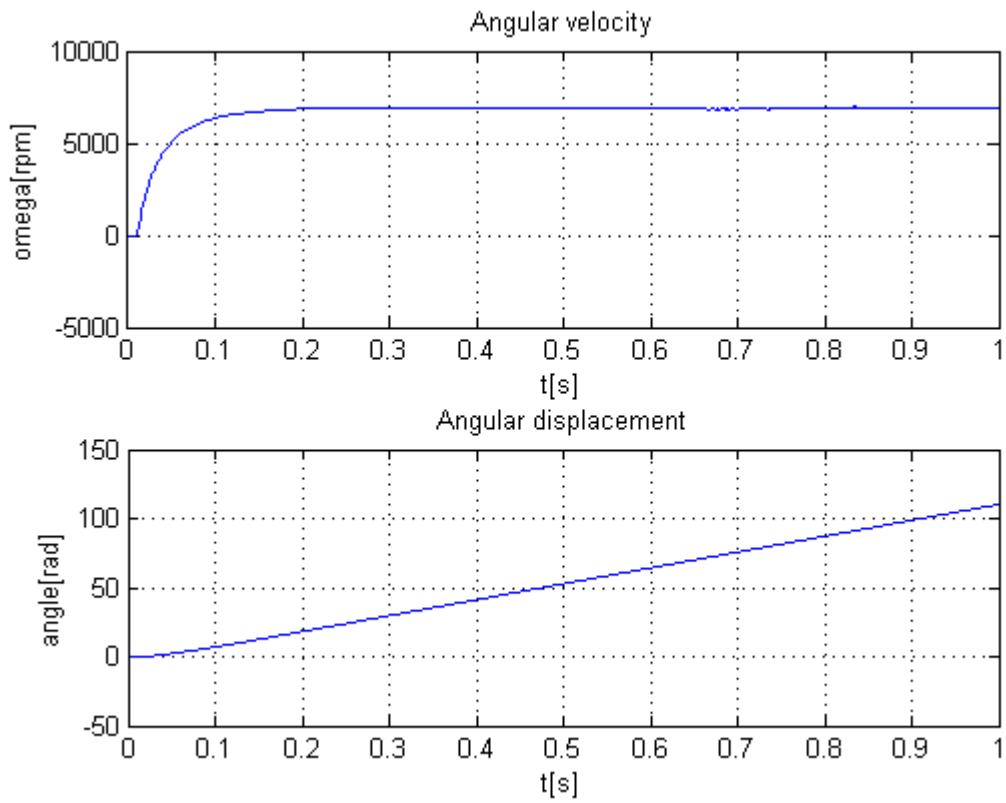
Figure 29 Angular velocity and displacement of the delta winding model

5 Hardware model of the BLDC

5.1 Purpose of the model

One of the parts of this thesis is creating a hardware model designated to evaluate the BLDC control units. There are several assembly lines in the company that manufacture products (pumps) that include a BLDC motor. Each of those products has to be tested before it is sold to the customer. Part of the inspection process is connecting the pump to a testbench, where the motor is started up and several parameters, like vibration, direction of the rotation, rate of flow and others are measured [32]. In order to be certain that we get correct outputs from the measurement, we have to know that the BLDC control unit is working properly and the same way as at the previous measurements. For this reason a reference part that does not change its electrical parameters is required. Unfortunately, a normal BLDC motor cannot be used for this application because the mechanical rotations change the response of the windings in time [32]. Furthermore, other parameters like viscous friction, angular speed or torque can change too. It is obvious that all those troubles are caused by the mechanical movement. That is why we wanted to create a device, which would contain no mechanical parts but would act similar to the real BLDC in the electrical way. In this way, the control unit would not recognize that a real BLDC is not connected to its output and it would send the usual control signals to the reference, which does not change its parameters so it would be possible to evaluate the unit's parameters.

In order to be able to work with the motors in the first place, I needed to gather as much information about the control units as possible (Chapter 5.2). Then in Chapter 5.3, hardware part of the model and its control software is described. Chapter 5.4 describes the means that have been used to evaluate the reference and compare it with real motors. Last part of this chapter then deals with evaluation of multiple customer's control units (CCU) on the reference and our internal control unit on a motor.

5.2 Evaluated control unit

For the main testing, I have obtained the customer's industrial control unit, which is installed directly to cars (Figure 30). The control principles and hardware schematics

of the unit were unfortunately not at my disposal. I have, however, obtained following data, vital for the control unit's settings:

Power supply

Supply voltage	9 – 16 V
Maximum current	14 A

Control PWM signal

Frequency	100 Hz
Duty cycle	

	No rotation	1 – 9 %
	Speed control	10 - 90 %
	Full speed	>= 90 %
	Error	100%
	Sleep	0 %

Error processing

Overheating	Switch off
Control error	Full speed
Current too high	Normal behaviour
Current too low	Full speed
Short-circuit	Switch off

It is necessary to say that this information is only unofficial and according to my experience with this unit is the reaction to the PWM control slightly different. Unfortunately we were not able to obtain any other information, above all about the control algorithm of the unit, which would be definitely very helpful. For this reason I could only anticipate the way the unit works from the literature I had. I only knew that it had to be some sort of sensorless delta winding control algorithm.
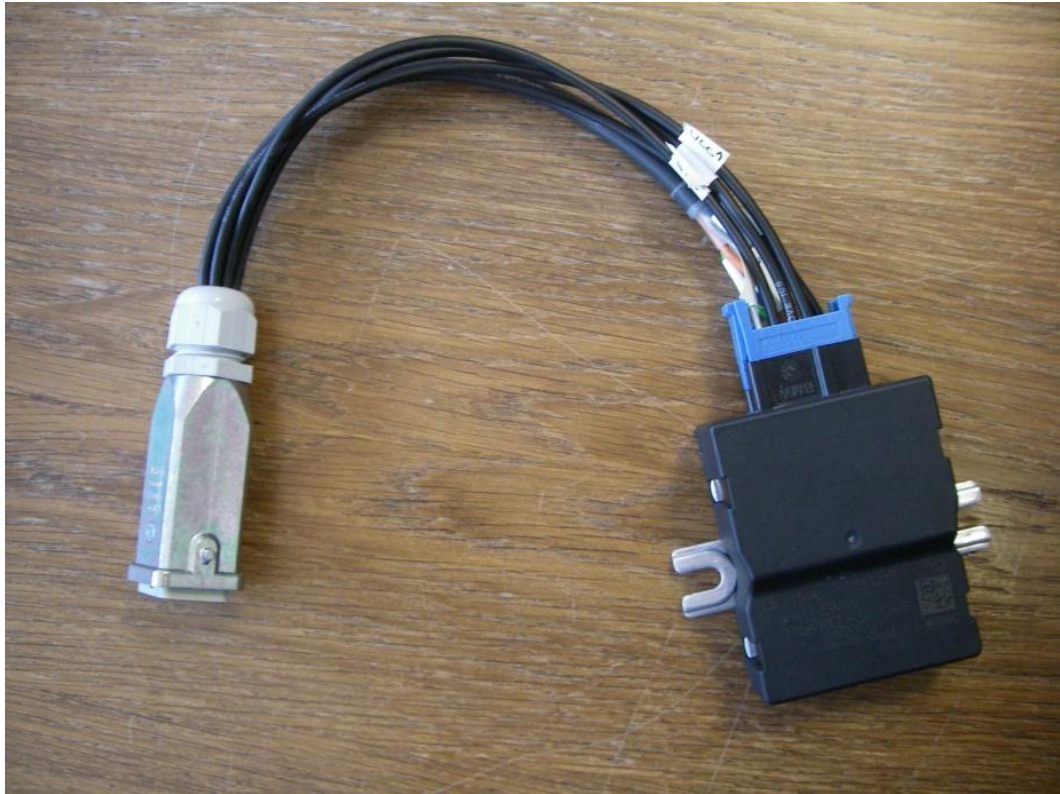
Figure 30 BLDC control unit

According to [2], a good way to control a delta winding motor without sensors is the Back EMF integration. This algorithm integrates the voltage over a 60 degrees period when the phase is disconnected from the supply voltage and from the ground. In the six-step motor control, one phase is measured twice in one control period. When the motor is stopped, there is no Back EMF affecting the voltage on the disconnected phase. The voltage is then half of the supply voltage. As soon as the motor starts rotating, a Back EMF emerges on the winding and is subtracted from the voltage on the free phase (Figure 31). By integrating this voltage, the algorithm obtains a positive or negative number indicating whether the motor speed is slower or faster than the commutation speed. If the speed is different from the desired speed, the algorithm adjusts a commutation frequency and changes the duty cycle of the output PWM. If the integrated number is zero, the motor is either steady (but then the voltage is constant) or the motor has reached the right speed.
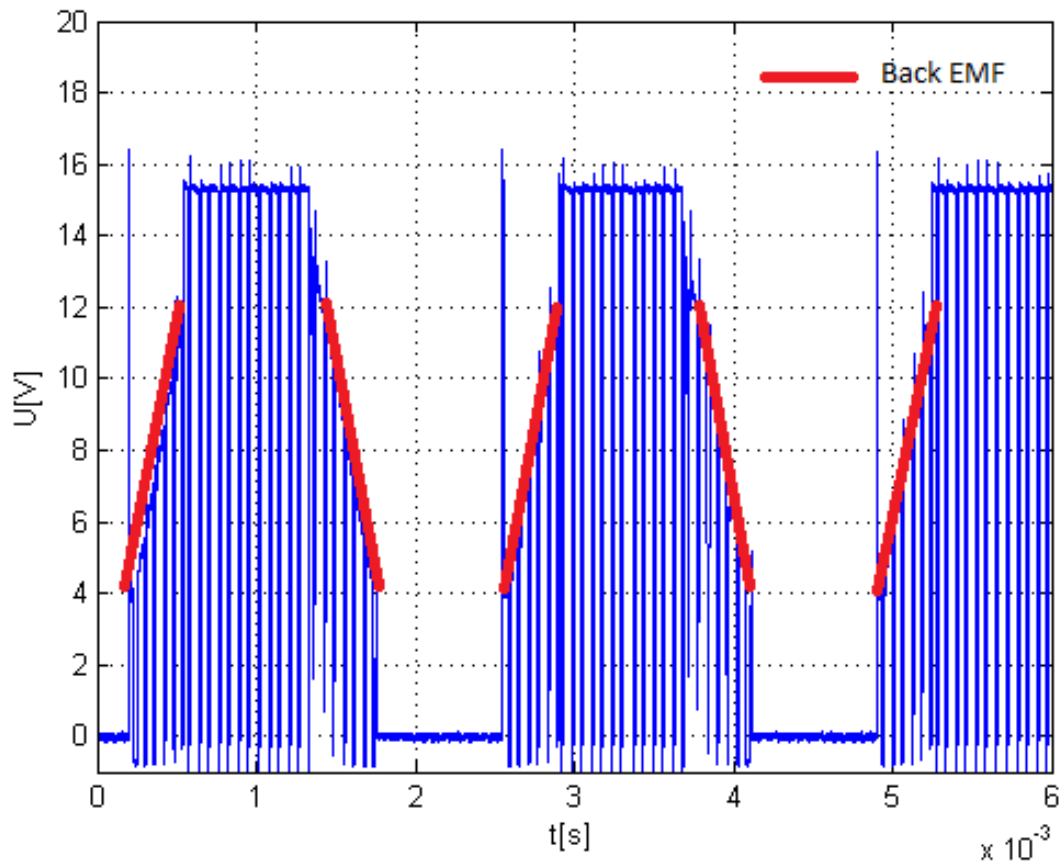
Figure 31 Back EMF integration period

For my testing, I have supposed that the unit uses the same or similar algorithm like the one I have described.

5.3 Design of the model

5.3.1 Hardware part

It is clear that the reference has to include a replacement of the winding to simulate an inductive load of the motor. After a short searching for a trio of inductors, which would have the same induction and resistance as each phase of the motor I have realized that the best way is to use windings from an original disassembled motor. Because of that I can be sure that the parameters of the windings are as close to the original as possible.

After this, I needed to find a way how to simulate the Back EMF. According to Lenz's Law, the polarity of the induced voltage always opposes the polarity of the supply voltage. This means that the Back EMF causes a reduction of a current flowing through the phase. A different way how to achieve this effect is to put a variable resistance, which would cause a similar current reduction, in series with the phase. This can be accomplished by connecting a transistor on each phase. Best type of transistor for this application is in my opinion a bipolar NPN transistor because it allows approximately a linear amplification. I have used a darlington pair so as to decrease a current consumption in the base. This allows me to connect basically any signal generation device to the input, because it has high impedance. Complete schema of the reference is in appendix C.
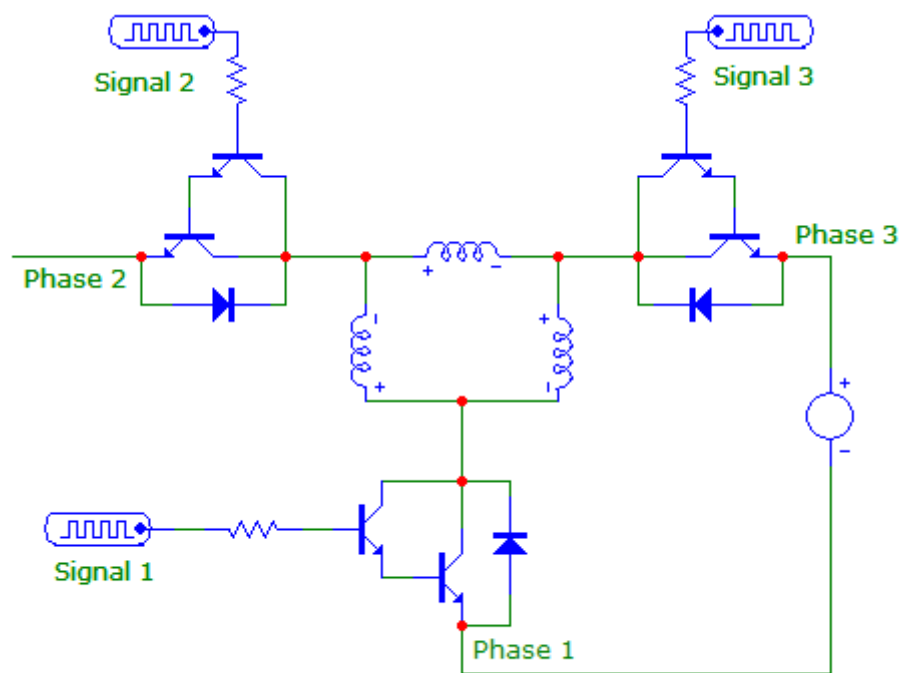
Figure 32 Schema of the reference in one control step

As shown in the Figure 32, there are three darlington pairs in the schema. Each darlington is connected to one phase. When the transistor's emitter is connected to the ground, which happens two times every six-step control period, it can be controlled via the current flowing through its base and emitter to the ground. This changes the voltage

division ratio of the two phases and the signal connected to the base appears on phase two. Signal on phase two does not appear just as signal on phase three, where the darlinton's pair is short-circuited by the diode connected anti-parallel to the transistors. Owing to this solution, I did not have to deal with stopping the signal on two remaining transistors and I was allowed to send the signal to all the three transistors continuously.

5.3.2   Signal generation

My first idea for the signal generation was a hardware feedback. My plan was to use a trio of passive RC integrators with their inputs connected to the control units output and their output connected to the bases of the transistors (Figure 33). This subcircuit would then integrate the signal and create a substitution of a Back EMF signal for the reference. Because of the phase delay, the output of one phase integrator had to be connected to a base of another phase's transistor, so the timing of the artificial field would be correct. I have tried this solution with a big range of the RC constant values, but unfortunately, none of them seemed to be able to simulate the Back EMF signal well enough for the control unit to accept it. This is why I had to try another way.
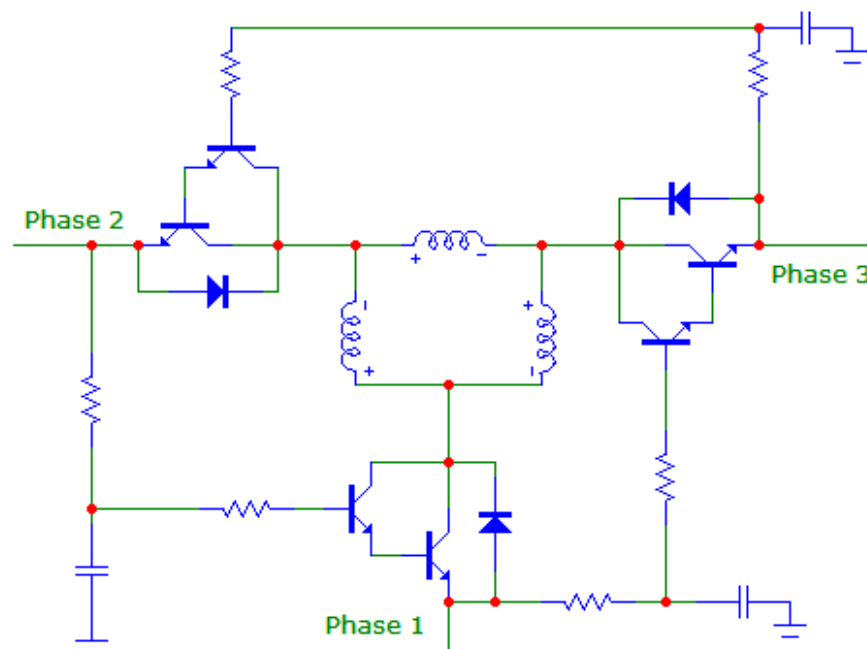

Figure 33 RC feedback control schema

Another solution that naturally emerged was to generate the Back EMF digitally. I have decided to use a platform by National Instruments. Since our company has an opened license for the LabView development software and number of digital NI cards able to read and generate analog signals I have decided to use this platform. For this task I have obtained NI CompactDAQ 4-Slot USB Chassis with two removable cards (Figure 34). First card was NI 9205 with 32 single-ended or 16 differential analog inputs, 16-bit resolution and 250 kS/s sampling rate. The second card was NI 9263 with four 100 kS/s analog outputs. I had to use two different cards because I needed three analog inputs to read the phase signals from the control unit and three analog outputs to generate the Back EMF signal for each phase. Unfortunately, none of the single cards available fulfilled this requirement.

Figure 34 NI CompactDAQ 4-Slot USB Chassis

I have planned to create a feedback software Back EMF signal generation. I was able to read the signals from the control unit and to generate an EMF via the transistors. The solution was to process the signals from the control unit and from the result create three signals which would be sent back to the reference. Because the signals from the control unit included a PWM modulation, I needed to calculate an approximate envelope of the signal. LabView has a special function for this but unfortunately, it was not included in the libraries I had installed. As a substitution I have used a low-pass filter

which did not generate a perfect envelope but was sufficient for my needs. After this step I have experimentally determined a proper threshold level so as to transform the signal to a symmetrical square signal. Via sample by sample numerical integration, I was then able to create a triangle signal with the same frequency and adjustable amplitude, which was suitable for the Back-EMF simulation (Figure 35).
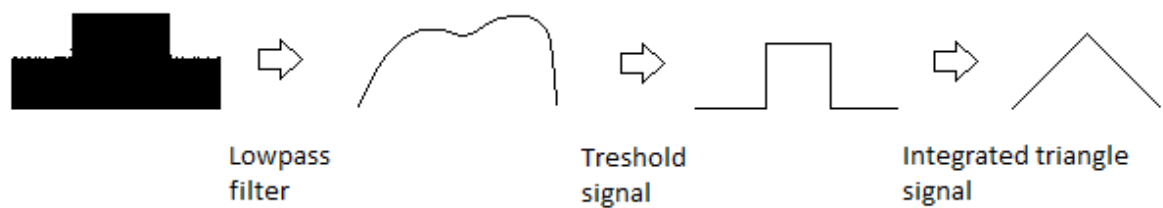

Lowpass filter

Treshold signal

Integrated triangle signal

Figure 35 Signal processing

Unfortunately, at this point another problem occurred. Both of the cards are able to run on sufficient frequency. However, the program, running under regular Microsoft Windows operating system, was not able to calculate the signal fast enough to supply the output card with proper data in time. The desired signal on the output then, of course, did not correspond with the calculation and the reference did not work.

For this reason, I had to come up with my final solution. Since the signal generation on this platform was not fast enough I have decided to use an open loop control. The output card is able to generate smooth signals up to 10 kHz. The condition is that its onboard clock must be used and the signal must be a periodical waveform. This way, the program just tells the card what kind of waveform to generate and the external hardware takes care of the rest. The idea was to generate a sine wave on each of the three outputs with phase shift of 120°. The frequency, offset and amplitude stay constant. This signal would be then used as an artificial Back EMF on the reference. When the signal is set, the control unit is connected. From its point of view, the motor is already rotating so it skips the part where it accelerates the motor and adjusts the phase switching to the artificial Back EMF frequency as fast as possible. It is necessary to mention that the control unit has its own desired speed derived from the control PWM. At first it tries to change the speed to this value. Of course, this cannot be achieved

because the Back EMF frequency is set by the external source. At this point, the control unit goes to a "control error mode", which means, it generates the maximum speed on its output. In the picture 36 and 37, this speed corresponds with the speed of the artificial Back EMF, the unit thinks that the motor is rotating and keeps generating the signals.
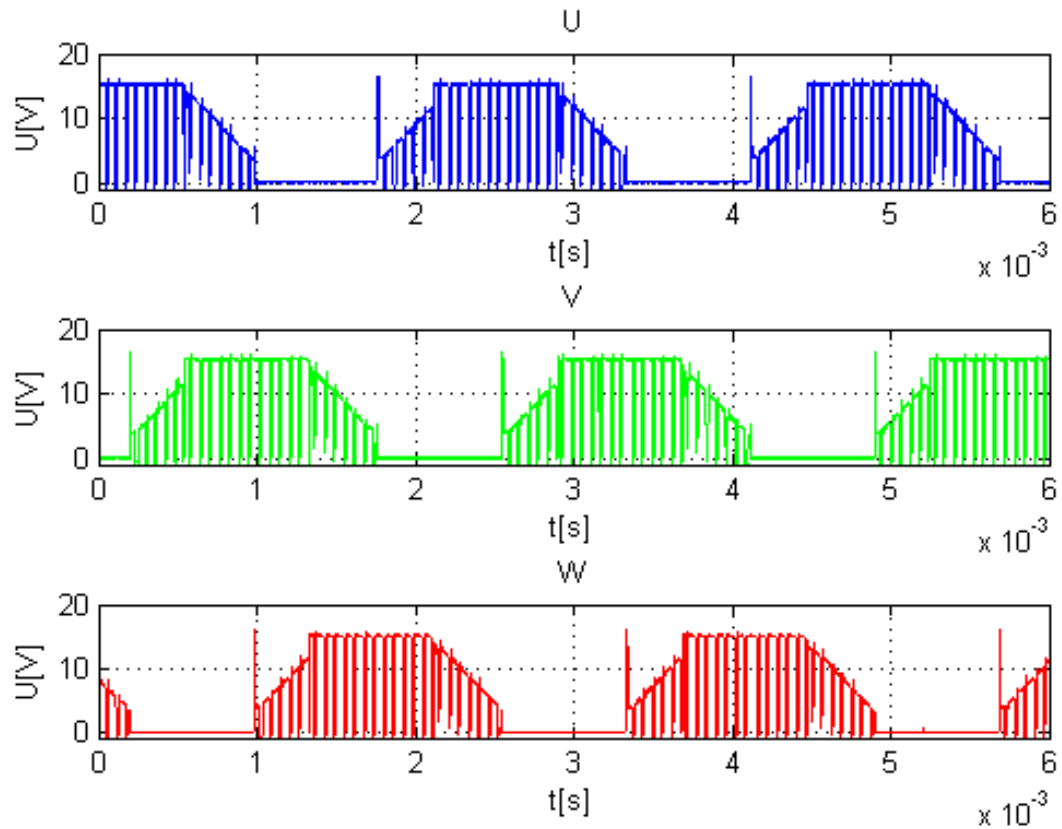

Figure 36 Full speed control unit signals

There are output signals of the control unit with and without the rotor in the picture 36 and 37. It is apparent that the signals do not look entirely the same. The rotor still creates a steady EMF field, which I was not able to fully imitate.

The duty cycle is different because the real motor cannot achieve the same maximum speed as the reference due to its physical limitations. However, for the testing purpose, the reference acts sufficiently similar to the original.
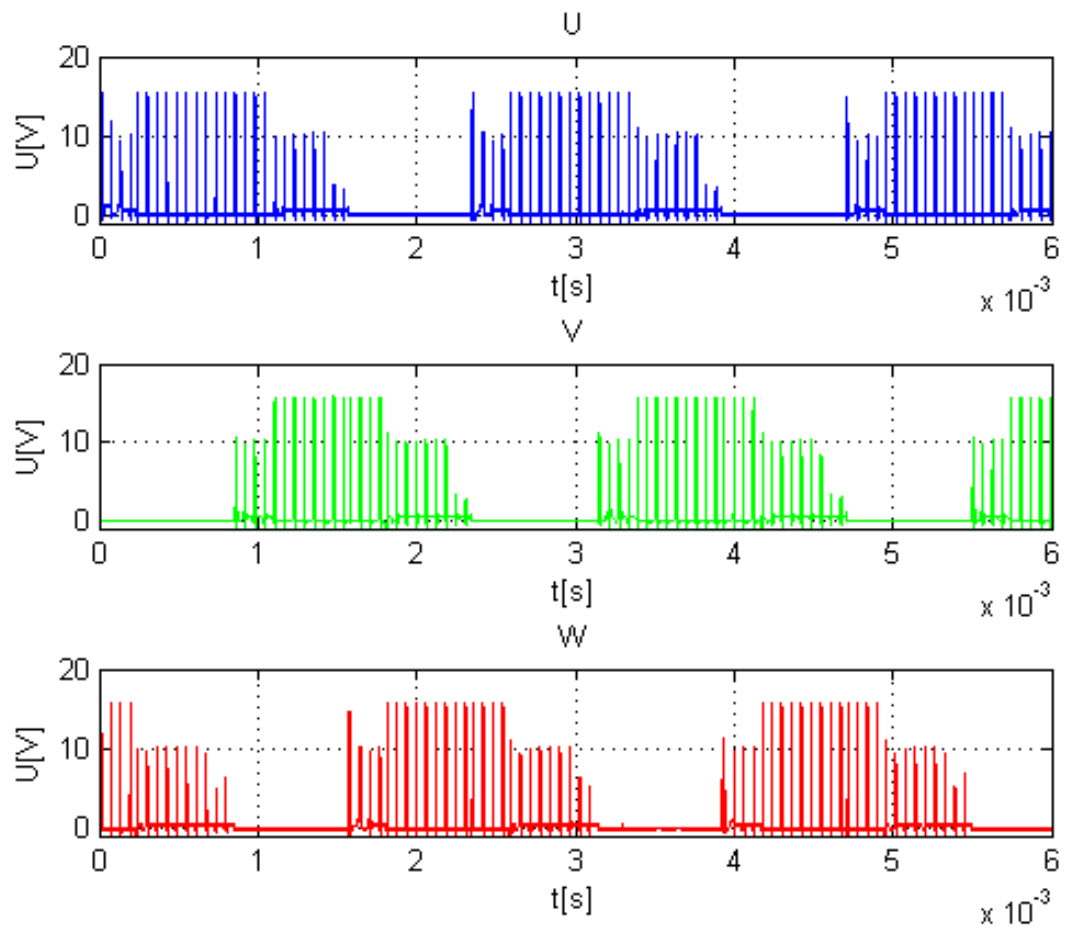
Figure 37 Full speed control unit signals with artificial Back EMF

5.3.3 Control program

As I have said, the software control environment was written in LabView programming language. I have chosen this language because it is designated for the external hardware I have used.
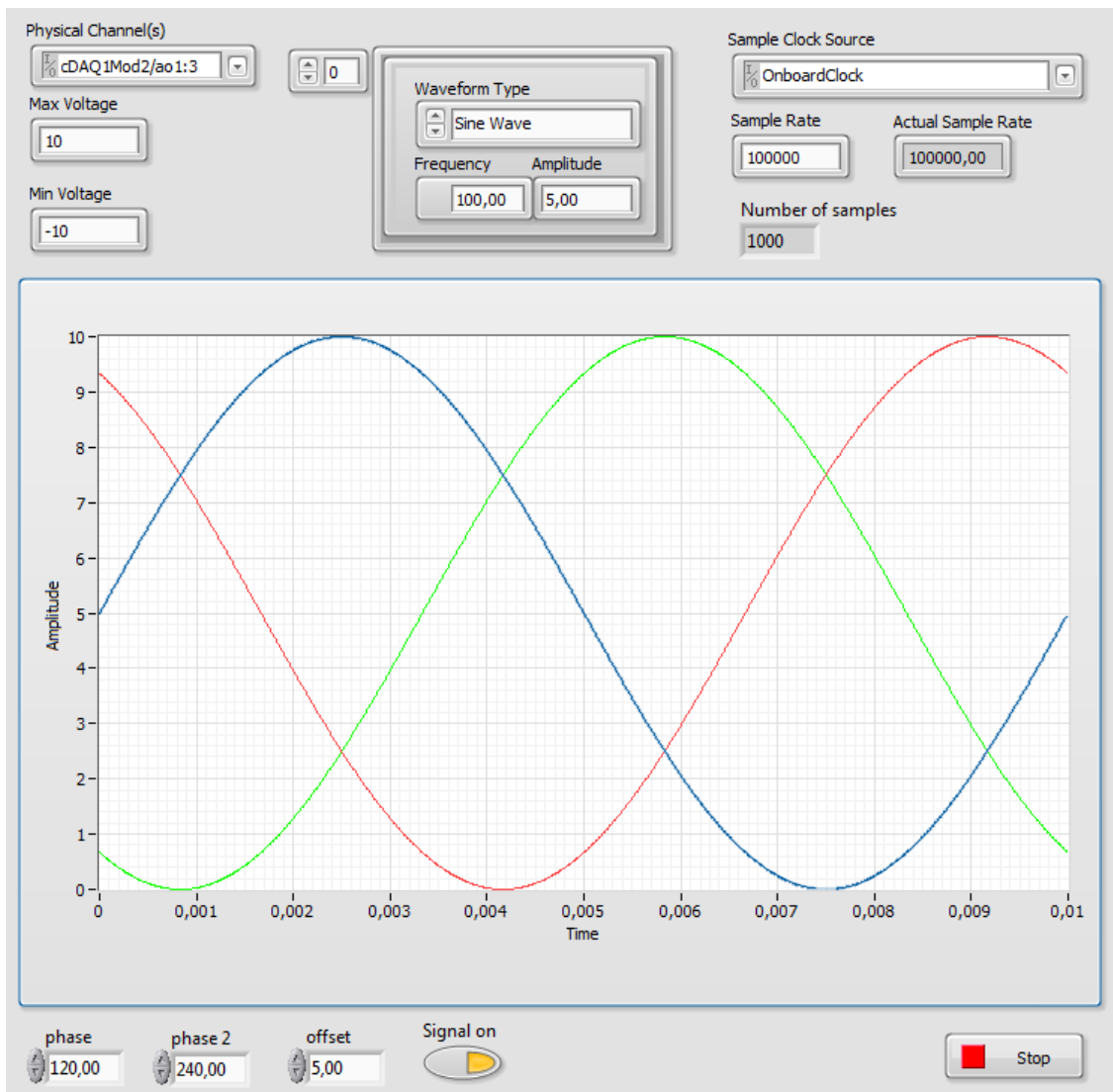
Figure 38 Control program interface

In the first step, parameters like physical channels, frequency, sample rate, amplitude, phase shift, offset and other are set. Those parameters are then processed in a for loop and transformed into three data vectors. After that, another loop follows where the data are continuously sent to the card's D/A converters. Since I needed to adjust the parameters while the program was running, I have included a subroutine in the loop waiting for the change, which restarts the main sequence when some parameters are modified. In the picture 38, there is the interface of the program. The structure of the program is available in Appendix A.

5.4 Model evaluation

In order to correctly evaluate the hardware model, I have performed measurement of the reference and three pumps for comparison. Each part was measured independently ten times so as to define its stability. I have measured the following parameters on each part: angular velocity, active power, RMS value of voltage on all phases, RMS value of current on all phases, power factor, apparent power, reactive power and efficiency. To measure the angular speed, I have measured frequency of one phase using an oscilloscope. The speed was then recalculated using formula (23).

$$\omega = \frac{f * 60}{number\ of\ poles} = f * 15 \tag{23}$$

Where
- ω[rad/s] is an angular velocity
- f [Hz] is the switching frequency

Rest of the values was measured using Norma 4000 Power analyser [15]. This measuring device is designed for measuring a great amount of parameters concerning electromechanical machines including those, I have mentioned. The pump was connected to the control unit according to figure 39.
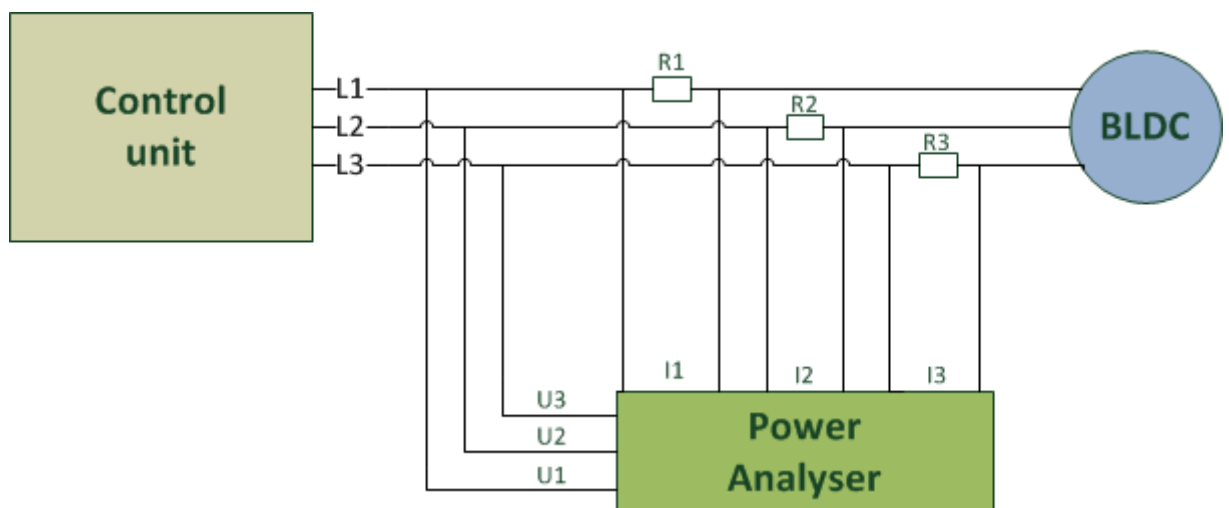

Figure 39 Connection of the measurement with the Power Analyser

The values are calculated via following formulas 24 – 30. Those are generally known equations. More detailed description is in [15]:

RMS Voltage [V]

$$U_{RMS} = \sqrt{\frac{1}{T} \int_0^T u^2 dt} \tag{24}$$

RMS Current [A]

$$I_{RMS} = \sqrt{\frac{1}{T} \int_0^T i^2 dt} \tag{25}$$

Active power [W]

$$P = \frac{1}{T} \int_0^T ui \, dt \tag{26}$$

Apparent power [VA]

$$S = U_{RMS} \, I_{RMS} \tag{27}$$

Reactive power [Var]

$$Q = \sqrt{S^2 - P^2} \tag{28}$$

Power factor [-]

$$\lambda = \frac{P}{S} \tag{29}$$

Efficiency [%]

$$\eta = 100 \frac{P_1}{P} \qquad\qquad (30)$$

It is obvious that Norma 4000 calculates the efficiency of the motor differently than it is usually calculated. Efficiency of the motor is defined as a ratio between power of the mechanical output and the input electrical power. In this case it is a ratio between power of one phase and power of all phases combined.

Figure 40 Measurement with Norma 4000

I have performed the first measurement on three pumps and the reference (Figure 40). Its goal was to determine the difference between individual parameters of the pumps

and the reference. Other task was to find the variance of those parameters and define which one is most suitable for further testing.

Pump 1	Revolutions [RPM]	Prms [W]	power factor	Urms[V]	Irms[A]	S [kVA]	Q [kVar]	Efficiency [%]
1	6375	10,4	0,42	7,22	1,12	0,023	0,021	33,1
2	6525	9,7	0,42	7,17	1,08	0,023	0,02	33,4
3	6315	9,6	0,41	7,15	1,08	0,023	0,021	33
4	6390	9,9	0,42	7,18	1,08	0,023	0,021	32,3
5	6480	9,8	0,42	7,17	1,07	0,022	0,02	32,9
6	6405	9,7	0,42	7,19	1,08	0,023	0,021	33,3
7	6405	9,9	0,42	7,2	1,1	0,023	0,021	33,1
8	6375	10,7	0,43	7,23	1,13	0,024	0,022	32,3
9	6450	9,8	0,42	7,16	1,07	0,023	0,02	32,7
10	6375	10,2	0,42	7,08	1,1	0,023	0,021	33,2
mean	6410	9,97	0,42	7,175	1,091	0,023	0,0208	32,93
min	6315	9,6	0,41	7,08	1,07	0,022	0,02	32,3
max	6525	10,7	0,43	7,23	1,13	0,024	0,022	33,4
variance	3287	0,1121	0,00002	0,001585	0,000389	2E-07	3,6E-07	0,1341

Pump 2	Revolutions [RPM]	Prms [W]	power factor	Urms[V]	Irms[A]	S [kVA]	Q [kVar]	Efficiency [%]
1	6315	9,44	0,42	7,15	1,05	0,02	0,022	32,8
2	6420	9,52	0,41	7,13	1,05	0,022	0,02	33,3
3	6480	9,2	0,41	7,14	1,05	0,022	0,02	32,4
4	6570	9,5	0,41	7,13	1,05	0,022	0,02	32,6
5	6420	10,63	0,41	7,22	1,13	0,024	0,022	32,1
6	6300	9,4	0,41	7,12	1,04	0,022	0,02	33
7	6330	9,6	0,42	7,13	1,05	0,022	0,02	32,7
8	6360	9,2	0,42	7,13	1,06	0,023	0,02	33,17
9	6480	9,8	0,42	7,14	1,06	0,022	0,02	32,9
10	6420	9,5	0,42	7,1	1,04	0,022	0,02	33
mean	6410	9,579	0,415	7,139	1,058	0,0221	0,0204	32,797
min	6300	9,2	0,41	7,1	1,04	0,02	0,02	32,1
max	6570	10,63	0,42	7,22	1,13	0,024	0,022	33,3
var	6572	0,150849	0,000025	0,000889	0,000616	8,9E-07	6,4E-07	0,117681

Pump 3	Revolutions [RPM]	Prms [W]	power factor	Urms[V]	Irms[A]	S [kVA]	Q [kVar]	Efficiency [%]
1	6570	9,98	0,42	7,2	1,09	0,023	0,021	32
2	6210	9,96	0,42	7,2	1,07	0,022	0,021	32,8
3	6375	9,9	0,42	7,16	1,08	0,023	0,021	32,9
4	6330	9,5	0,41	7,16	1,06	0,023	0,02	33,2
5	6495	9,2	0,41	7,15	1,05	0,022	0,02	32,3
6	6360	9,5	0,42	7,15	1,06	0,022	0,02	32,8
7	6390	9,3	0,41	7,12	1,05	0,022	0,02	33,2
8	6435	9,9	0,42	7,18	1,08	0,23	0,21	32,9
9	6345	10,4	0,43	7,2	1,12	0,024	0,021	32,7
10	6450	10,1	0,41	7,14	1,05	0,022	0,02	33,4
mean	6396	9,774	0,417	7,166	1,071	0,0433	0,0394	32,82
min	6210	9,2	0,41	7,12	1,05	0,022	0,02	32
max	6570	10,4	0,43	7,2	1,12	0,23	0,21	33,4
var	8784	0,131124	4,1E-05	0,000704	0,000449	0,003873	0,003234	0,1596

Reference	Revolutions [RPM]	Prms [W]	power factor	Urms [V]	Irms [A]	S [kVA]	Q [kVar]	Efficiency [%]
1	1500	1,8	0,24	10,21	0,24	0,007	0,007	34
2	1500	1,81	0,24	10,2	0,25	0,007	0,007	34,1
3	1500	1,85	0,24	10,2	0,26	0,007	0,007	33,5
4	1500	1,82	0,24	10,18	0,24	0,007	0,007	33,7
5	1500	1,78	0,23	10,18	0,25	0,007	0,007	34,1
6	1500	1,8	0,23	10,16	0,24	0,007	0,007	34,3
7	1500	1,83	0,23	10,11	0,24	0,007	0,007	34,2
8	1500	1,8	0,23	10,12	0,25	0,007	0,007	34,1
9	1500	1,82	0,24	10,09	0,25	0,007	0,007	34
10	1500	1,8	0,24	10,11	0,24	0,007	0,007	33,9
mean	1500	1,811	0,236	10,156	0,246	0,007	0,007	33,99
min	1500	1,78	0,23	10,09	0,24	0,007	0,007	33,5
max	1500	1,85	0,24	10,21	0,26	0,007	0,007	34,3
var	0	0,000349	2,4E-05	0,001784	4,4E-05	0	0	0,0509

Table 5 Initial measurement on three pumps and the reference

I have performed only 10 measurements on each pump due to the high time requirements of this test and limited time on the analyser. All four units were controlled by one customer's control unit. The motors were tested on the unit's maximum speed. The reference was supplied with 100 Hz artificial Back EMF, which means that its apparent rotational speed was 1500 rpm. Unfortunately, the speed of the motors and the reference could not be the same, because the motors had troubles with the rotation stability on lower speed and the reference suffered from heat stability problems on higher frequencies.

According to Table 5, all units had a very low variance of power factor, apparent power and reactive power. The pumps had all very unstable rotational speed. The reference, however, had a variance zero, because the results were all the same. This is caused by the absence of the shaft and by the fact, that the speed is defined only by the frequency of artificial Back EMF. Thanks to that, the instability of the reference speed is beyond my measurement capabilities. Also the variance of the reference's power is lower by three orders.

Considering the meaning of the values themselves, we can confirm that the pumps act like an inductive load because of the average power factor 0,4 and reactive power more than 20 Var. Even more interesting is the fact, that the power factor is lower by one half by the reference.

According to the results, I have defined the parameters revolutions and active power as key parameters for the evaluation. The company has a well-established procedure how to evaluate the measurement quality. First, the mean value ($\bar{X}_g$) and standard deviation (S_g) of the measurement is calculated. Then the tolerance (T) must be set. With all those values, a crucial parameter C_g can be computed (31). If its value is greater than 1,33 it means that 98% of the results lie in the tolerance zone and the process is correct. Otherwise, the process is unfit.

$$C_g = \frac{0,2\,T}{6\,S_g} \tag{31}$$

For each parameter, I have set the tolerance so the motor with the best variance has the C_g value precisely 1,33. This way, the rest of the motors had to be out of the

tolerance zone and easy to compare with the reference via the C_g parameter. Since the mean values were significantly different, I had to recalculate the tolerance for the reference with the proper ratio. In both cases, the best variance had motor 1. In case of the active power, the C_g value of the reference was 4,08. This means that the stability of active power is much better by the reference. Even better result is in case of the revolutions stability. Since all the values were the same in case of the reference, the C_g was impossible to calculate, because the program would have to divide by zero. It is obvious, that the reference defeated the motors in this category as well. Example of the C_g calculation protocol is in Appendix B.

It is necessary to add that the real power stability is highly dependent on the heat stability of the transistors at the reference. This is the reason why I was forced to regularly cool the reference with 6-bar flowing air. So as to find out how much the heat influences the stability, I have performed a 12 minutes long measurement, when the reference was running without any rest and monitored changes of the power.
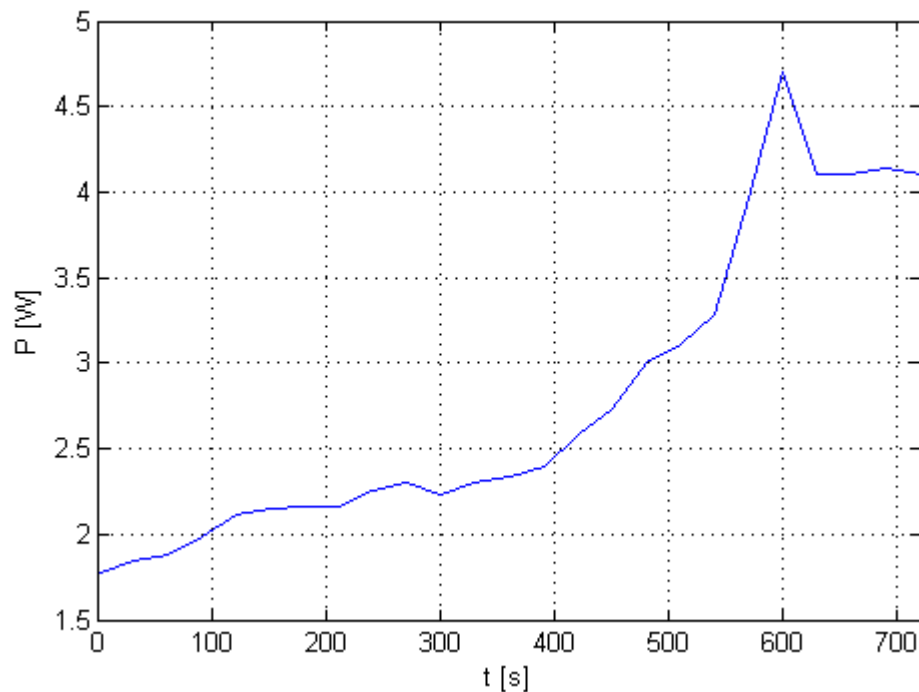
Figure 41 Heat test measurement of the reference

It is apparent from the picture 41 that the heat significantly affects the value of this parameter. For this reason I was forced to use the air-flow cooling. In the future, the

heat influence could be reduced by parallel tripling the transistors on each phase. That would reduce the power on each transistor three times and also significantly decrease their heat load. Of course, additional passive or active heat sink would be used too. Unfortunately, the air-flow cooling, which is very effective, cannot be applied for a practical use.

5.5 Control unit evaluation

I have used a similar procedure for evaluating the Control units as I have in the previous chapter. I have obtained three customer's control units and the task was to figure out, which one is the best. The units were tested on the hardware reference on the parameters active power [W] and reactive power [Var]. Except those two, also power factor, apparent power [VA] and efficiency [%] were measured. The apparent angular velocity of the shaft was defined by the reference – 1500 RPM.
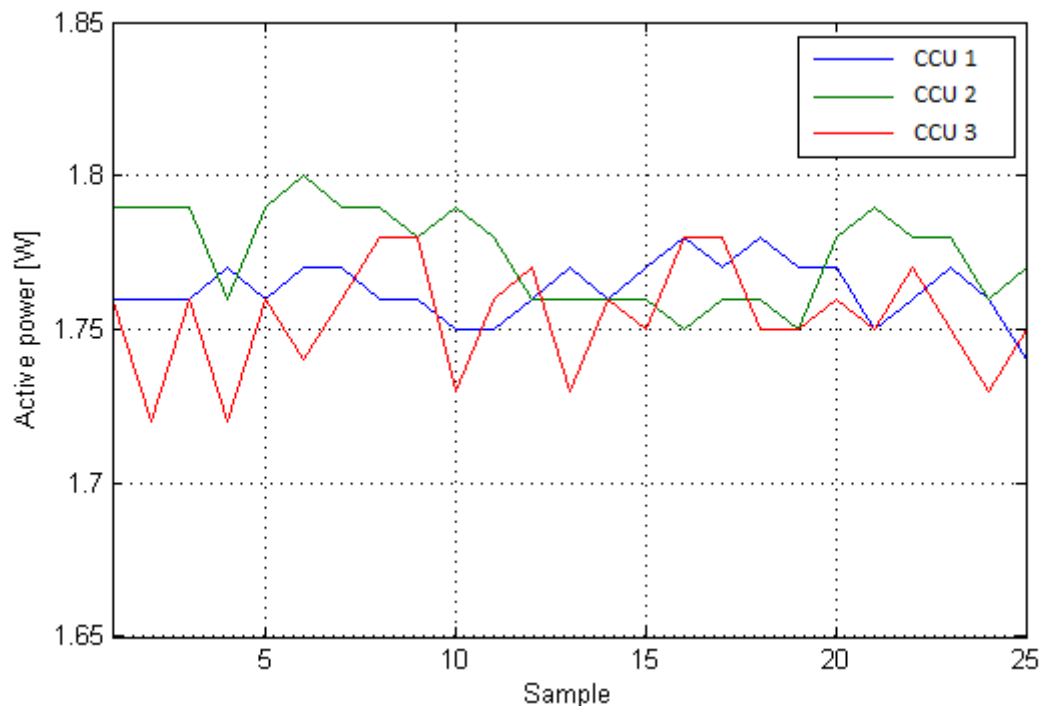
Figure 42 Active power measurement

In both cases, CCU 1 had the lowest variance: 8,576E-05 W and 0,0024 Var. For this reason, I have defined the tolerance zone so that CCU 1 exactly fits into it (C_g=1,33). In the table 6 are the C_g values for both parameters of all three control units.

	P stability [Cg]	Q stability [Cg]
CCU 1	1,33	1,33
CCU 2	0,85	1,01
CCU 3	0,7	0,57

Table 6 Stability evaluation
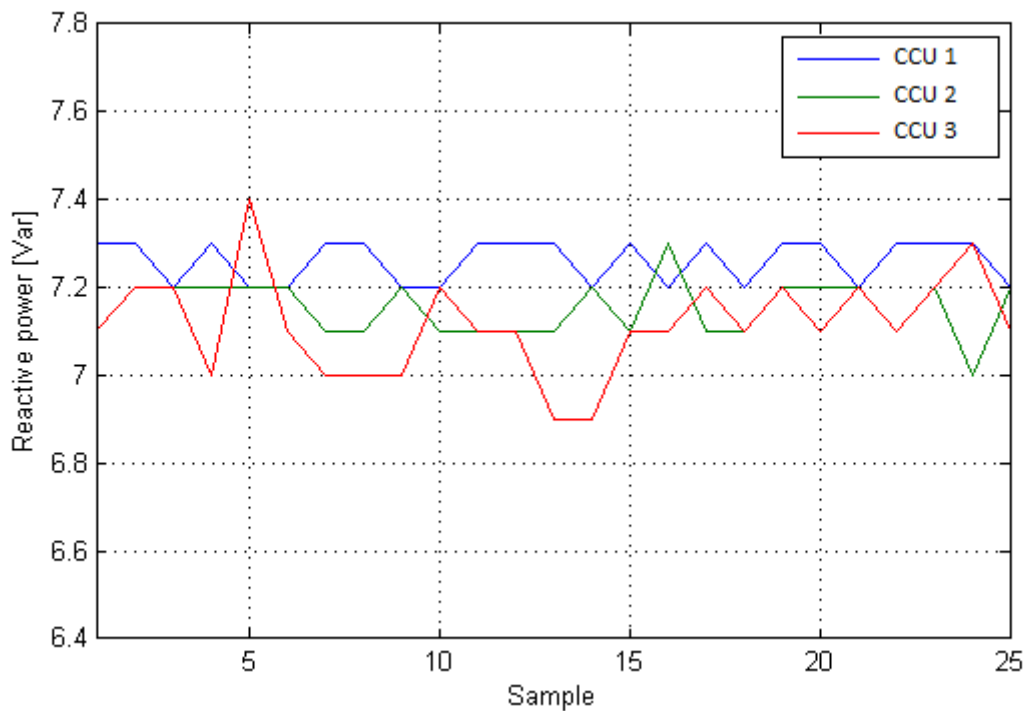
Figure 43 Reactive power measurement

In general, I can afford to say that all the units act very similar. According to Table 7, all CCUs have relatively low variance for all parameters. CCU 3 had the lowest mean reactive power but also the lowest apparent power which corresponds with the fact that this unit has also slightly lower real power. Although this value is not so different, in

this point of view we can say that CCU 3 is the best unit, because it consumes less power while maintaining the same angular velocity of the shaft. On the other hand, in case of stability, CCU 1 would be the best choice. However, most important fact is, that this kind of control units appears to be valid for a wider use in the production.

CCU 1	P[W]	Power factor	S[Va]	Q[Var]	Efficiency[%]
mean	1,76	0,24	7,48	7,26	32,89
max	1,78	0,24	7,50	7,30	33,50
min	1,74	0,23	7,40	7,20	32,30
median	1,76	0,24	7,50	7,30	32,90
variance	0,000086	0,000002	0,001344	0,002400	0,115136

CCU 2	P[W]	Power factor	S[Va]	Q[Var]	Efficiency[%]
mean	1,77	0,24	7,37	7,15	32,73
max	1,80	0,24	7,50	7,30	33,10
min	1,75	0,23	7,30	7,00	32,40
median	1,78	0,24	7,40	7,20	32,70
variance	0,000225	0,000002	0,003776	0,004096	0,040416

CCU 3	P[W]	Power factor	S[Va]	Q[Var]	Efficiency[%]
mean	1,75	0,24	7,35	7,12	33,58
max	1,78	0,24	7,60	7,40	34,50
min	1,72	0,23	7,10	6,90	33,10
median	1,76	0,24	7,40	7,10	33,50
variance	0,000312	0,000003	0,009696	0,012544	0,118624

Table 7 Statistical evaluation of the control units

Apart from the customer's control units, we also have our internal control unit, (ICU), which is currently being withdrawed from the production due to troubles with the starting sequence. I was asked to compare this unit with the customer's unit to find out, how it stacks up against it. Unfortunately, ICU does not work with the reference. For this reason, I have tested the units on motor 1. The units controlled the motor so it would rotate approximately on 6300 RPM. Power factor, efficiency, active, apparent and reactive power have been measured 25 times.

CCU 3	P[W]	Power factor	S[Va]	Q[Var]	Efficiency[%]
mean	9,39	0,41	22,62	20,49	33,64
max	9,61	0,42	22,90	20,60	34,00
min	9,20	0,41	22,30	20,10	33,00
meadian	9,40	0,42	22,70	20,50	33,70
variance	0,006511	1,6256E-06	0,021824	0,019456	0,069504

ICU	P[W]	Power factor	S[Va]	Q[Var]	Efficiency[%]
mean	9,13	0,51	17,53	15,05	33,18
max	9,73	0,52	18,40	15,70	34,00
min	8,66	0,50	16,90	14,60	32,20
median	9,15	0,51	17,30	14,90	33,20
variance	0,090999	1,24544E-05	0,210816	0,115296	0,129376

Table 8 Comparison of CCU 3 with ICU

It is apparent that despite the starting sequence problem, ICU has in general better parameters than the customer's control unit. Its average power factor is about 10% higher, which means that it has better apparent-reactive power ratio, lower average active power and that it consumes less energy. However, in spite of those advantages, the problems with starting are still more significant and fatal for further usage of this unit.
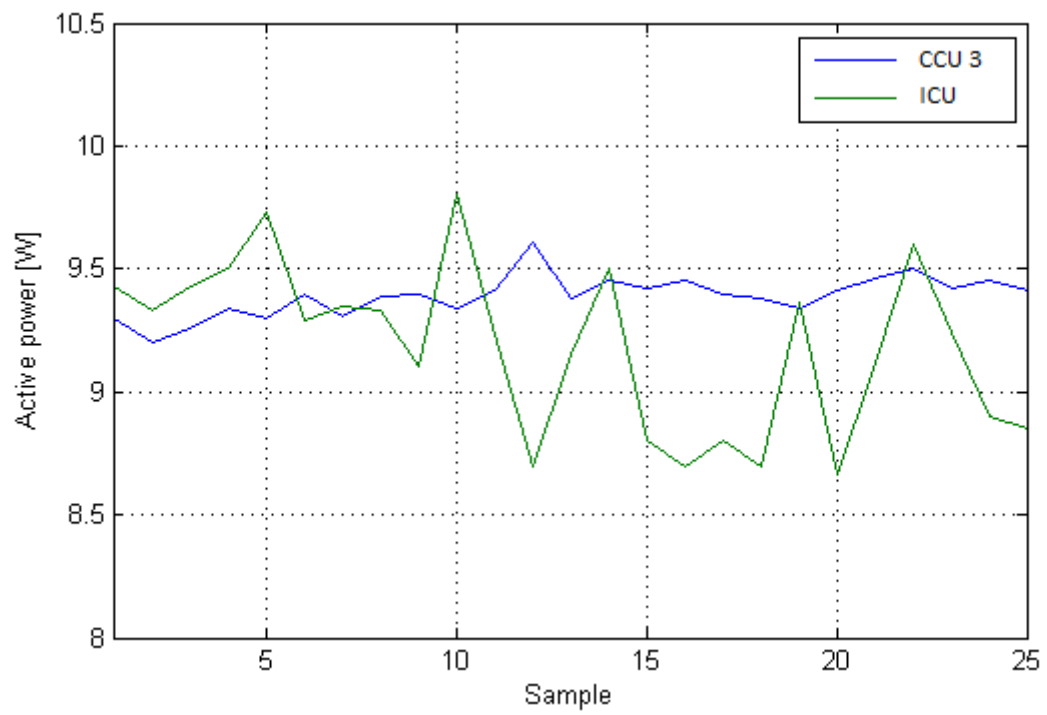
Figure 44 Active power of CCU and ICU

6 Conclusion

Purpose of this thesis was to find out current issues in the area of modeling of the BLDC motors and their application in medicine (Chapter 3). First I have dealt with the specific requirements of the medical environment on the BLDC motors (Chapter 3.1). Next step was to map current possibilities in the domain of computer simulation of electrical machines. I have described three development tools: Matlab Simulink, Modelica and NI electric motor simulation toolkit (Chapter 3.3). The first one is a well known tool representing the causal data flow graphical programming. By connecting blocks representing basic or more complex mathematical operations with signal wires, it is possible to simulate most of the linear and non-linear systems. The final comparison is summarized in Chapter 3.3.5 and Table 3.

Next step was creating a software model of the BLDC motor. Based on the results in Chapter 3.3, I have chosen Matlab Simulink as my simulation tool. First it was necessary to describe the motor mathematically (Chapter 4.1). For a complete model, it was also essential to obtain all the required constants. I have performed number of tests in order to be able to simulate the motor as precisely as possible (Chapter 4.2). As far as the model itself is concerned, I had to make two of them. First is a star winding BLDC, second one is a delta winding BLDC motor. More usual is the star winding version but because our motor was in a delta connection, I was forced to come up with this version as well.

Last part of this thesis was a construction of a BLDC hardware reference designated for evaluation of our industrial control units. First task was to compare the reference with three motors used in our company. The results showed that the reference had much more stable angular speed and also better active power stability. Its disadvantage is its tendency to heat up after a constant work (Chapter 5.4). This can, however, be avoided by using more parallel control transistors and by automation of the measurement process, which would shorten the running cycle to the order of seconds.

For evaluation of the BLDC control unit, I have obtained three customer's units. In general, all the units were very similar, which is very important for their application to the manufacturing process. In the stability's point of view, CCU 1 is the best choice.

Another important parameter is the active power on the reference. In this discipline CCU 3 is the best unit. However, the differences were very small and negligible for the purpose of our use.

The last comparison was between the CCU and other control unit, currently being put aside, ICU. Unfortunately, this unit did not work with the reference due to the instability of the phase output (Chapter 5.5). For this reason I was forced to measure both of them on a common BLDC motor. I have found out that although it has some serious issues with starting up the motors, the ICU's power factor is approximately 10% lower, which means it consumes less power with the same output. On the other hand, its stability of active power came out significantly worse.

List of figures

List of tables

List of quotes

[1] Rizanaliah Kasim. Khairatul Akmal. *Modeling and Simulation of Brushless DC Machines*. Faculty of Electrical Engineering. University of Technical Malaysia. Melaka 2012

[2] Jianqi Qiu, Cenwei Shi. Sensorless Control of Brushless DC Motor with Delta Connection Windings. In: *Electrical Machines and Systems (ICEMS* [online]. China: IEEE, 2010. [vid. 5.5.2014]. ISBN: 978-1-4244-7720-3.

 [3] Jiří Skalický, *Elektrické regulované pohony* [online], Fakulta elektrotechniky a komunikačních technologií, VUT, Brno, 2007 [vid. 5.5.2014]. Available from: www.vutbr.cz/www_base/priloha.php?dpid=18964

[4] AOIPuk, *Programmable micro-ohmmeter OM 21*, datasheet

[5] FLUKE PM 6306, *A versatile 1 MHz component measurement system*, datasheet

[6] Michael Bloom. *Medical devices aided by the BLDC motor*. Sinotech. Infographic. 2013

[7] Irvine Sloan, *Brushless dc Electric Motors Within Medical Applications*, NMB Technologies Corp., 2009, [vid. 5.5.2014]. Available from: http://www.nmbtc.com/motors/white-papers/motors_emergence_of_brushless_dc.html

[8] *Ventricular Assist Devices (VAD)* [online]. UCSF Department of Surgery. Available from: http://www.surgery.ucsf.edu/conditions--procedures/ventricular-assist-devices-%28vad%29.aspx

[9] *BLDC Motor Control for Respirators - Using high-speed sensorless BLDC motor control in medical device* [online]. Freescale. Datasheet. Available from: http://cache.freescale.com/files/32bit/doc/brochure/BBBLDCMCRSPTRART.pdf

[10] ABL800 FLEX Analyzer. In: Radiometer Medical [online]. [vid. 5.5.2014]. Available from: http://www.radiometer.com/en/products/blood-gas/abl800-flex-analyzer

[11] *Medical application solution* [online]. Allied Motion Technologies Inc. Products overview. Available from: http://www.alliedmotion.com/Data/Documents/catalogs/AMMedical_R1%28web%29.pdf

[12] *Treatment Methods for Kidney Failure: Hemodialysis*. National Kidney and Urologic Diseases Information Clearinghouse (NKUDIC). [vid. 14.4.2014]. Available from: http://kidney.niddk.nih.gov

[13] Power Wheelchair. In: SelfCare Home Health Products Ltd. [online]. [vid. 17.4.2014]. Available from: http://www.selfcarehome.com/ProdCategory/Wheelchairs%20-%20Power

[14] Padmaraja Yedamale, *Brushless DC (BLDC) Motor Fundamentals* [online], Microchip Technology Inc. 2003. Available from: http://electrathonoftampabay.org/www/Documents/Motors/Brushless%20DC%20%28B LDC%29%20Motor%20Fundamentals.pdf

[15] Fluke. *Norma 4000/5000 Power Analyser*. Operators Manual

[16] Jiří Kofránek, Pavol Privitzer, Marek Mateják, Martin Tribula,. *Akauzální modelování – nový přístup pro tvorbu simulačních her*. ÚPF 1. LF UK. Praha. 2009. ISSN: 1803-8115

[17] *High-Performance Electric Motor Simulation Using the NI Electric Motor Simulation Toolkit*. National Instruments [online]. [vid. 29.3.2014]. Available from: http://www.ni.com/white-paper/13778/en/.

[18] Atmel Corporation, *Sensor-based control of three phase brushless DC motor*, Application note, 2013

[19] Transformer Star and Delta Configurations. In: Zone4Info [online]. Available from: http://zone4info.com/articles/print/507/format/smoothbox

[20] Hrabovcová, V. Rafajdus, P. Franko, M. Hudák, P. *Meranie a modelovanie elektrických strojov*. Žilina: Žilinská univerzita, 2004. 335 s. ISBN 80-8070-229-2.

[21] A. Tashakori, M. Ektesabi, N. Hosseinzadeh - *Modeling of BLDC Motor with Ideal Back-EMF for Automotive Applications*. London. 2011. ISBN 978-988-19251-4-5

[22] Miroslav Ložek, Pavel Zahradník, Jan Havlík. *Regulace BLDC pohonů pro asistivní technologie*. Praha

[23] Abdel-Karim Daud. *Brushless D.C. Motor For Medical Applications*, Palestine Polytechnic University. 2010. ISBN: 978-960-474-209-7

[24] Mark S. Slaughter, M.D., *Advanced Heart Failure Treated with Continuous-Flow Left Ventricular Assist Device*, Massachusetts Medical Society, 2009

[25] *What is Ventricular Assist Device?* [online]. National Heart, Lung and Blood institute [vid. 25.5.2014]. Available from: http://www.nhlbi.nih.gov/health/health-topics/topics/vad/

[26] *What is Sleep Apnea* [online]. National Heart, Lung and Blood institute [vid. 25.4.2014]. Available from: http://www.nhlbi.nih.gov/health/health-topics/topics/sleepapnea/

[27] *Sleep apnea* [online]. American Sleep Apnea Association [vid. 27.4.2014]. Available from: http://www.sleepapnea.org/learn/sleep-apnea.html

[28] *CPAP* [online]. Joey Devilla [vid. 27.4.2014]. Available from: http://www.joeydevilla.com/2008/04/09/cpap-or-snorkeling-while-i-sleep/

[29] *Medical analyzer* [online]. Nanjing Everich Medicare [vid. 12.3.2014]. Available from: http://www.everichmed.com/

[30] *New dental tech obliterates drill sounds* [online]. T3 [vid. 13.3.2014]. Available from: http://www.t3.com.au/2011/01/11/new-dental-tech-obliterates-drill-sounds/

[31] *Dental drill* [online]. How products are made [vid. 28.3.2014]. Available from: http://www.madehow.com/Volume-3/Dental-Drill.html

[32] *VB_13022*. Bosch internal report. 2013

[33] Václav Vrána, Stanislav Kocman. *Stejnosměrné stroje* [online]. Katedra obecné elektrotechniky. FEI VŠB-TU Ostrava. 2004

[34] *Matlab Simulink* [online]. Mathworks [vid. 5.4.2014]. Available from: http://www.mathworks.com/products/simulink/
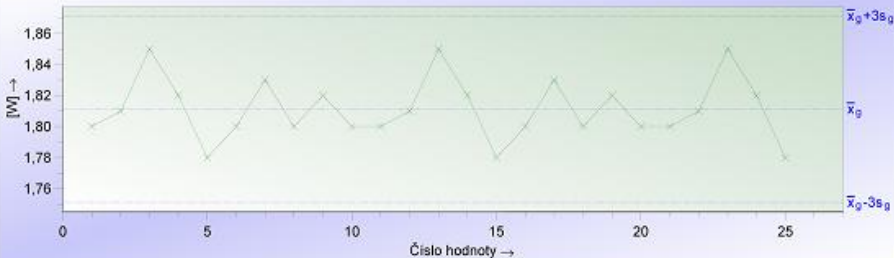
[35] *Modelica* [online]. Modelica and the Modelica Association [vid. 5.4.2014]. Available from: https://www.modelica.org/

[36] Ricardo Cmapla, Elio Torres, Francisco Salas, Víctor Santibanez. *On Modeling and Parameter Estimation of Brushless DC Servoactuators for Position Control Tasks*. *Instituto Tecnol´ogico de la Lagun,*. Mexico. 2012

Appendix A - Schema of the NI program
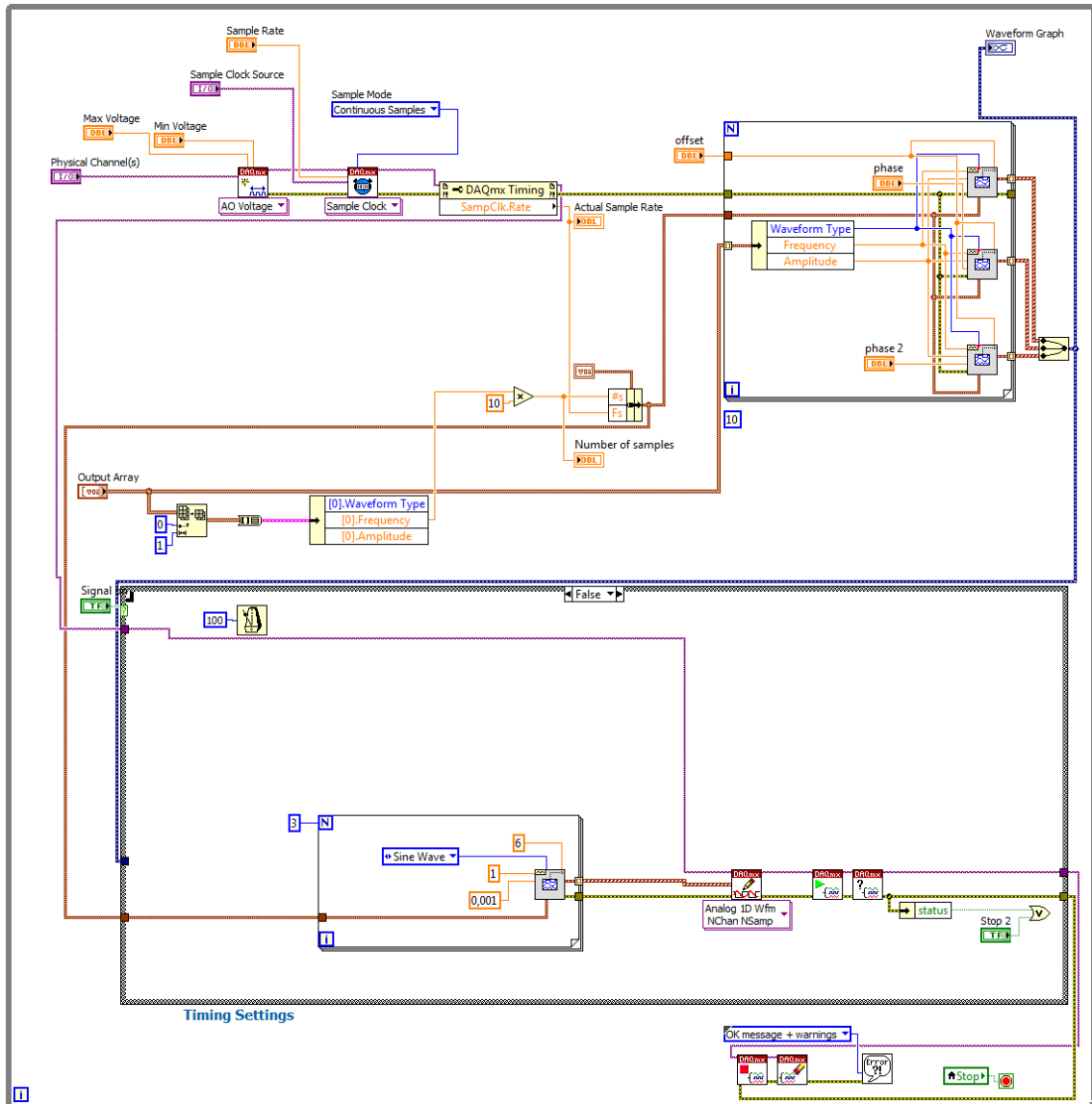
Appendix B – Example of the Bosch measurement approval protocol

Appendix C – Schema of the reference and values of the components
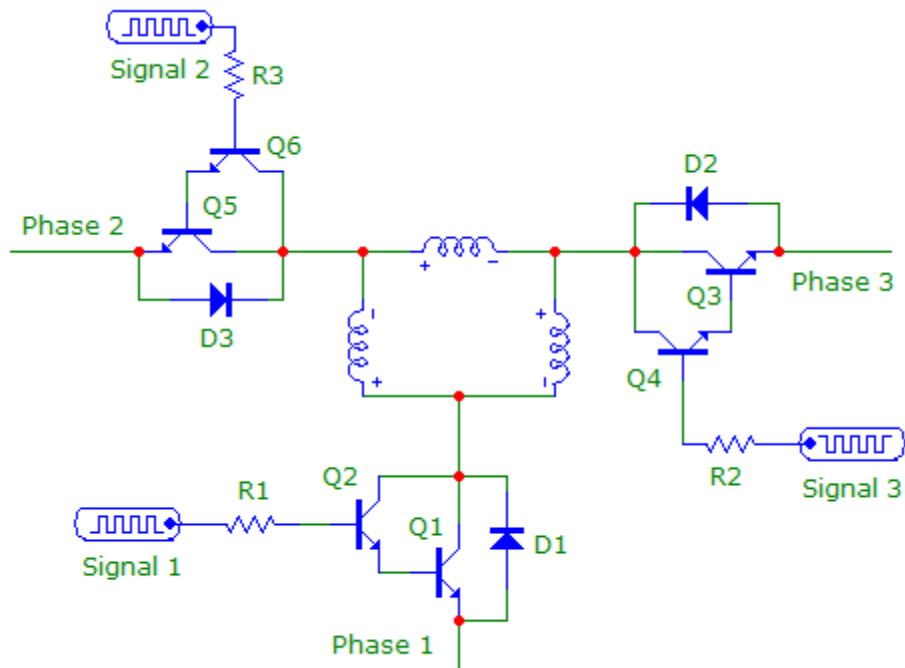
Part	Value	Device	Description
D1,D2,D3	-	1N4007	Diode
Q1, Q2, Q3, Q4, Q5, Q6	-	BD911	NPN Transistor
R1, R2, R3	20k	-	Resistor

Appendix D – Contents of the attached CD

The root folder of the CD contains three subfolders:

- **thesis** – contains a .pdf file with the thesis
- **software_model** – contains the Matlab software model of the BLDC
- **hardware_model** –contains the control program for the hardware model